Adv Polym Sci (2020) 285: 21–62
https://doi.org/10.1007/12_2019_53

Published online: 10 April 2020

How to Design Both Mechanically Strong and Self-Healable Hydrogels?

Oguz Okay

Contents

Abstract Several strategies have been developed in the past decade for the fabrication of self-healing or self-recovery hydrogels. Because self-healing and mechanical strength are two antagonistic features, this chapter tries to answer the question "How to design both mechanically strong and self-healable hydrogels?". Here, I show that although autonomic self-healing could not be achieved in high-strength hydrogels, a significant reversible hard-to-soft or first-order transition in cross-link domains induced by an external trigger creates self-healing function in such hydrogels. I mainly focus on the physical hydrogels prepared via hydrogen-bonding and hydrophobic interactions. High-strength H-bonded hydrogels prepared via self-complementary dual or multiple H-binding interactions between hydrophilic polymer chains having hydrophobic moieties exhibit self-healing capability at elevated temperatures. Hydrophobic interactions between hydrophobically modified hydrophilic polymers lead to physical hydrogels containing hydrophobic associations and crystalline domains acting as weak and strong cross-links, respectively. Semicrystalline self-healing hydrogels exhibit the highest mechanical strength reported so far and a high self-healing efficiency induced by heating above the melting temperature of the alkyl crystals. Research in the field of self-healing hydrogels provided several

O. Okay (✉)
Department of Chemistry, Istanbul Technical University, Istanbul, Turkey
e-mail: okayo@itu.edu.tr

important findings not only in the field of self-healing but also in other applications, such as injectable gels and smart inks for 3D or 4D printing.

Keywords Hydrogels · Hydrogen-bonding interactions · Hydrophobic associations · Mechanical properties · Self-healing · Semicrystalline hydrogels

Abbreviations

β_o	CTAB/AAc molar ratio in the gelation solution
η_o	Zero-shear viscosity
ε	Strain
ε_f	Fracture strain
$\dot{\varepsilon}$	Strain rate
λ	Deformation ratio
$\lambda_{biax,max}$	Maximum biaxial extension ratio
λ_{max}	Maximum deformation ratio
ν_e^{dry}	Cross-link density
ξ_H	Hydrodynamic correlation length
σ_f	Fracture stress
σ_{nom}	Nominal stress
ω	Frequency
AAc	Acrylic acid
AAm	Acrylamide
AMPS	2-Acrylamido-2-methyl-1-propanesulfonic acid
BAAm	N,N′-Methylenebis(acrylamide)
C12M	Dodecyl methacrylate
C17.3M	Stearyl methacrylate
C18A	N-Octadecyl acrylate
C22A	Docosyl acrylate
CNFs	Cellulose nanofibrils
C_o	Initial monomer concentration
CTAB	Cetyltrimethylammonium bromide
DAT	Diaminotriazine
DMAA	N,N-Dimethylacrylamide
DMSO	Dimethyl sulfoxide
DNA	Deoxyribonucleic acid
E	Young's modulus
EtBr	Ethidium bromide
f_ν	Fraction of associations broken during the loading
G'	Storage modulus
G''	Loss modulus
GO	Graphene oxide
MAAc	Methacrylic acid
NAGA	N-Acryloyl glycinamide

NIPAM	N-Isopropylacrylamide
PAAc	Poly(AAc)
PAAm	Poly(AAm)
PAMPS	Poly(AMPS)
PDMAA	Poly(DMAA)
PEG	Poly(ethylene glycol)
PVP	Poly(N-vinylpyrrolidone)
SDS	Sodium dodecyl sulfate
SFS	Scanning force microscopy
tan δ	Loss factor ($=G''/G'$)
T_m	Melting temperature
U_{hys}	Hysteresis energy
UPy	Ureidopyrimidinone
WLMs	Worm-like micelles

1 Introduction

Hydrogels are 3D networks of chemically and/or physically cross-linked polymer chains swollen in water. They are soft and smart materials with a variety of applications including superabsorbents, tissue engineering, drug delivery, soft contact lenses, and so on [1–4]. Because the first-generation classical hydrogels prepared using a chemical cross-linker were too weak or brittle in nature, extensive studies conducted in the past decade explored a new design principle for the fabrication of mechanically strong hydrogels of high toughness [5–12]. This principle bases on creating an effective energy dissipation in the hydrogel network using sacrificial or reversible bonds that prevent propagation of crack and hence a catastrophic damage even under large strain. Otherwise, that is, if the crack energy localizes around the crack tip and cannot be dissipated as in the classical hydrogels, rapid crack propagation leads to the fracture of the whole hydrogel. By manipulating the gel structure to induce dissipative mechanisms at the molecular level, the second-generation hydrogels developed so far exhibit Young's moduli and tensile strengths in the range of MPa and hence are a good candidate for the replacement of load-bearing tissues such as cartilage, tendons, and ligaments [2]. For example, double-networking strategy developed by Gong and co-workers bases on creating two interpenetrated and interconnected networks in a single hydrogel material, namely, highly and loosely chemically cross-linked polymer networks acting as brittle and ductile components, respectively [6, 13]. The sacrificial bonds of the brittle network break under a low strain to produce many microcracks by dissipating energy, while the ductile network keeps the macroscopic sample together.

Another important challenge emerging in the field of mechanically robust hydrogels is to generate self-healing or self-recovery ability in these materials. Self-healing, which is an inherent property of many biological systems, is defined

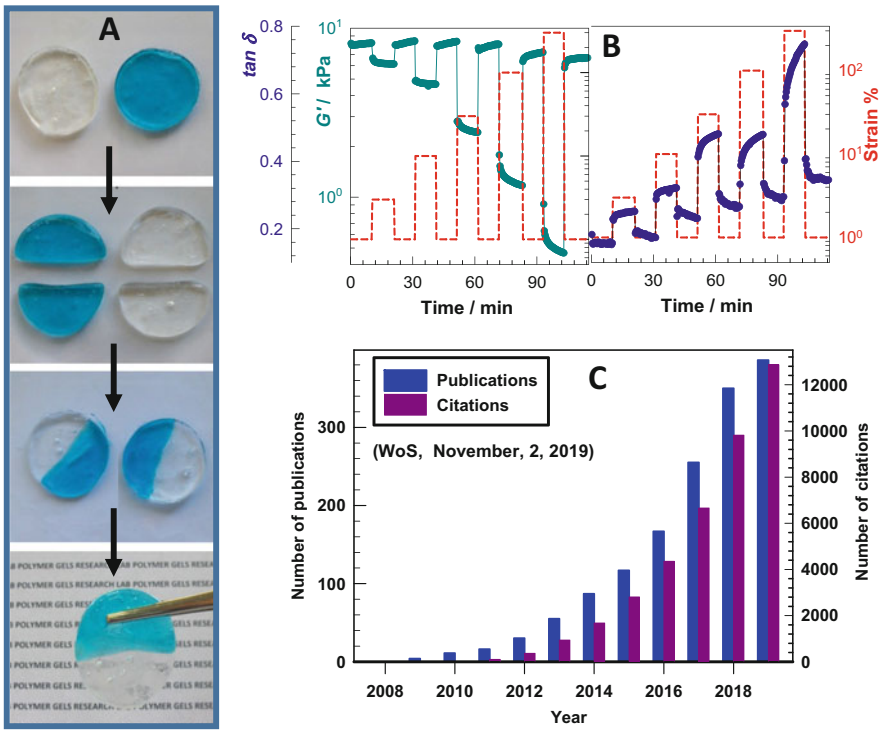

Fig. 1 (**a**, **b**) Cut-and-heal test (**a**) and on-off strain cycles (**b**) to monitor the self-healing and self-recovery capability of hydrogels, respectively. In (**a**), the images of two hydrophobically modified hydrogel specimens are shown; one of them was colored for clarity. After cutting the specimens into two parts followed by bringing the cut surfaces together, they merge to form their original shapes. From [14] with permission from the American Chemical Society. In (**b**), the storage modulus G' and the loss factor tan δ ($=G''/G'$, G'' is the loss modulus) of a nanocomposite DNA/clay hydrogel are shown as a function of the test time. The test consists of strain cycles composed of a stepwise increased high strain (from 2 to 300%) separated with a low strain (1%), as shown by the dashed red lines. Temperature = 25°C. From [15] with permission from the American Chemical Society. (**c**) The number of publications and citations with keywords "self-healing" or "self-recovery" and "hydrogels" according to the ISI Web of Knowledge portal on November 2, 2019. The total numbers of papers and citations are 1,478 and 39,613, respectively

as the capability of a material to heal macroscopic cracks such as cuts or scratches autonomously or under the effect of a stimulus such as the temperature. Thus, self-healing requires reformation of all bonds broken in a material to recover its original shape and mechanical properties. Although self-healing and self-recovery have sometimes been used synonymously, self-recovery more refers to cases of repairing internal microcracks in a material remaining externally intact after damage. Thus, cut-and-heal tests and rheological measurements have generally been conducted to monitor the efficiency of self-healing and self-recovery, respectively (Fig. 1a, b) [14, 15]. Self-healing is a highly desirable property for commercial polymers because it extends their lifespan and also reduces the burden of waste polymers

such as microplastics causing serious pollution in the seas [16]. It is also important for hydrogels as they are used as biomaterials, scaffolds in tissue engineering and drug delivery systems, and superabsorbents where their extended service time is of prime importance.

The number of the works published on self-healing/self-recovery hydrogels has grown almost exponentially during the past 10 years (Fig. 1c). Several reviews have been published covering exhaustive collection of all results reported so far [17–24]. A critical survey over the published works reveals that many studies deal with the preparation of self-healing physical hydrogels exhibiting a frequency-dependent low storage modulus and a Young's modulus and fracture stress in the Pa to kPa range. Because self-healing and mechanical strength are inversely related, it is not surprising to detect self-healing in such weak hydrogels having short-lived cross-links. However, hydrogels with a good mechanical performance such as cartilage require existence of cross-links with long lifetimes together with an efficient energy dissipation mechanism to prevent crack propagation. Because self-healing efficiency decreases with increasing lifetime of cross-links, it seems a challenge to generate self-healing in high-strength hydrogels with modulus and tensile strength in the range of MPa. This review tries to answer the question "How to design both mechanically strong and self-healable hydrogels?".

The capability to self-heal in hydrogels is generated by forming a reversible 3D network of polymer chains via dynamic covalent bonds or non-covalent interactions. Thus, instead of chemical cross-links, intermolecular bonds with finite lifetimes are used to build a hydrogel network. The type of the physical bonds and their lifetimes are key elements determining many of the properties of self-healing physical hydrogels. Dynamic covalent bonds such as phenylboronic ester, acylhydrazone, disulfide, dynamic imine bonds, as well as reversible radical and Diels-Alder reactions have been used to create self-healing in hydrogels. One may expect that such bonds will combine the strength and reversibility of covalent and non-covalent bonds, respectively. However, hydrogels formed via dynamic covalent bonds generally exhibit insufficient mechanical properties for load-bearing applications, and their preparation often requires sophisticated synthetic procedures [17]. Therefore, this review covers publications on creating mechanically strong self-healing/self-recovery hydrogels via non-covalent interactions. We focus here on hydrophobic and hydrogen-bonding interactions as well as on their combinations with ionic interactions. Self-healable polyampholyte hydrogels formed via ionic bonds [25], and physical double-network hydrogels have been reviewed by Sun and Cui in this volume [26].

Because of the inverse proportionality between self-healing efficiency and lifetime of intermolecular cross-links, one may argue that an effective self-healing could not be achieved in a mechanically strong hydrogel with long-lived cross-links. However, it could be achieved in a short period of time if an external trigger induces a significant, reversible hard-to-soft, or first-order transition from order to disorder in the cross-link domains of the hydrogels leading to a dramatic change in the cross-link lifetime. For example, if a semicrystalline physical hydrogel with a modulus and tensile strength in the MPa range is damaged, heating the damaged region above the

melting temperature T_m of crystal cross-links induces almost three orders of magnitude decrease in the modulus in that region so that, after cooling below T_m, the released crystallizable groups reform in that area to recover the original mechanical properties [27]. Thus, independent on the mechanical properties of hydrogels, self-healing requires a significant reversible softening in the damaged area induced by an external stimulus providing an enhanced mobility to the network chains.

A prerequisite for the preparation of tough and self-healing hydrogels is to reduce their water content to a moderate level, generally between 50 and 70 wt%. This is mainly due to the decrease in the polymer concentration of the hydrogels as the water content is increased leading to a reduced viscoelastic energy dissipation between the polymer chains inducing a tough-to-brittle transition. In addition, at high water contents, the polymer chains are already stretched due to the swelling pressure of water so that their further stretchability under an external force and hence tensile strength reduce significantly. For example, superabsorbent hydrogen (H)-bonded hydrogels in their as-prepared state with 65% water exhibit 1,000% stretchability and complete self-healing efficiency, whereas, in equilibrium swollen state with 99.9% water, they become brittle in tension and lack of self-healing [28]. The water content also affects the strength of the non-covalent bonds between the polymer chains in the hydrogel network. The strength of H-bonds between proteins, nucleic acids, or hydrophilic polymers in an aqueous environment is known to be much weaker than the H-bonds between water molecules. This weakening effect arises due to the fact that the formation of a H-bond between two polymers requires disruption of their H-bonds with water. To hinder the weakening of intermolecular interactions between polymers, mechanically robust and self-healable hydrogels reported so far generally have a water content between 50 and 70 wt%, which is, in fact, similar to that in living cartilage, skin, tendons, and ligaments [2].

2 H-Bonding Interactions

Because H-bonds between polymer chains are easily disrupted by water molecules and hence not stable in an aqueous environment, several strategies have been developed to create mechanically strong H-bonded hydrogels. These strategies mainly base on creation of self-complementary dual or multiple H-bonding interactions between polymer chains as well as incorporation of hydrophobic segments into the hydrophilic polymers to amplify the H-bonding interactions. The use of H-bond acceptor and donor comonomers in the hydrogel preparation, dual amide groups, ureidopyrimidinone units, and diaminotriazine-diaminotriazine interactions has been reported to create high-strength H-bonded hydrogels.

Inspired by nature such as the double and triple H-bonds in double-stranded deoxyribonucleic acid (DNA), stronger H-bonding interactions in hydrogels can be generated by using polymer chains having arrays of H-bonding sites. Because dual amide H-bonds are quite stable as compared to a simple amide H-bond, Liu and co-workers prepared hydrogels based on N-acryloyl glycinamide (NAGA), a

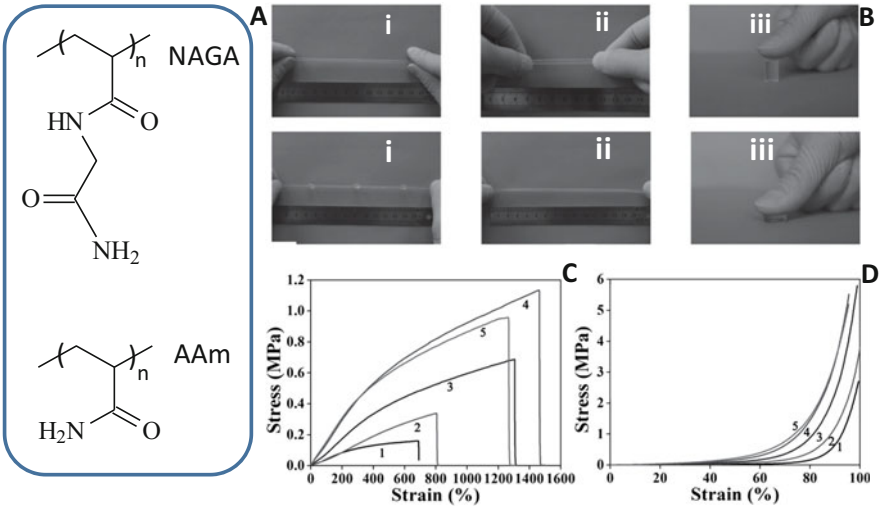

Fig. 2 (**a**) Structure of NAGA and AAm units. (**b**) Images of H-bonded hydrogel specimens formed at 25 wt% NAGA during knotting (i), during stretching (ii), and under loading (iii). (**c**, **d**) Tensile (**c**) and compressive stress-strain curves (**d**) of the hydrogels formed at various NAGA concentrations as indicated. NAGA concentrations = 10 (1), 15 (2), 20 (3), 25 (4), and 30 wt% (5). Figure 2b–d, from [29] with permission from Wiley

glycinamide-conjugated polymerizable monomer with dual amide in one side group (Fig. 2a) [29]. Photopolymerization of aqueous NAGA above 10 wt% concentration without a chemical cross-linker leads to physical hydrogels exhibiting good mechanical properties (mechanical strength, MPa level; stretch at break, ~1,400%) together with an excellent fatigue resistance (Fig. 2b–d) [29, 30]. This improved mechanical performance as compared to hydrogels derived from the monomers like acrylamide with a simple amide H-bond was attributed to the effect of stable multiple H-bonding domains serving as physical cross-links. NAGA hydrogels also exhibit thermoplasticity, remoldability, recyclability, reusability, and a high self-healing efficiency. The healing of a damaged NAGA hydrogel at 90°C for 3 h provides a healing efficiency of around 80%, i.e., the healed hydrogel sustains tensile stresses up to 1 MPa. During heating, the H-bonds at the cut region are disrupted so that the released H-bond donor and acceptor groups reform new H-bonds at the cut interface leading to healing of the NAGA hydrogels [29].

Incorporation of diaminotriazine (DAT) groups as the side chains into a hydrophilic polymer backbone also produces high-strength hydrogels due to the DAT-DAT interactions forming H-bonded dimers or higher-order aggregates [31–34] (Fig. 3a). It was shown that the DAT groups provide a hydrophobic microenvironment in hydrogels leading to strengthened DAT-DAT interactions in water. The ureidopyrimidinone (UPy) units developed by Meijer et al. are popular building blocks able to form self-complimentary dimers with quadruple H-bonds [35]. Although the dimer activity of UPy decreases in hydrophilic environment,

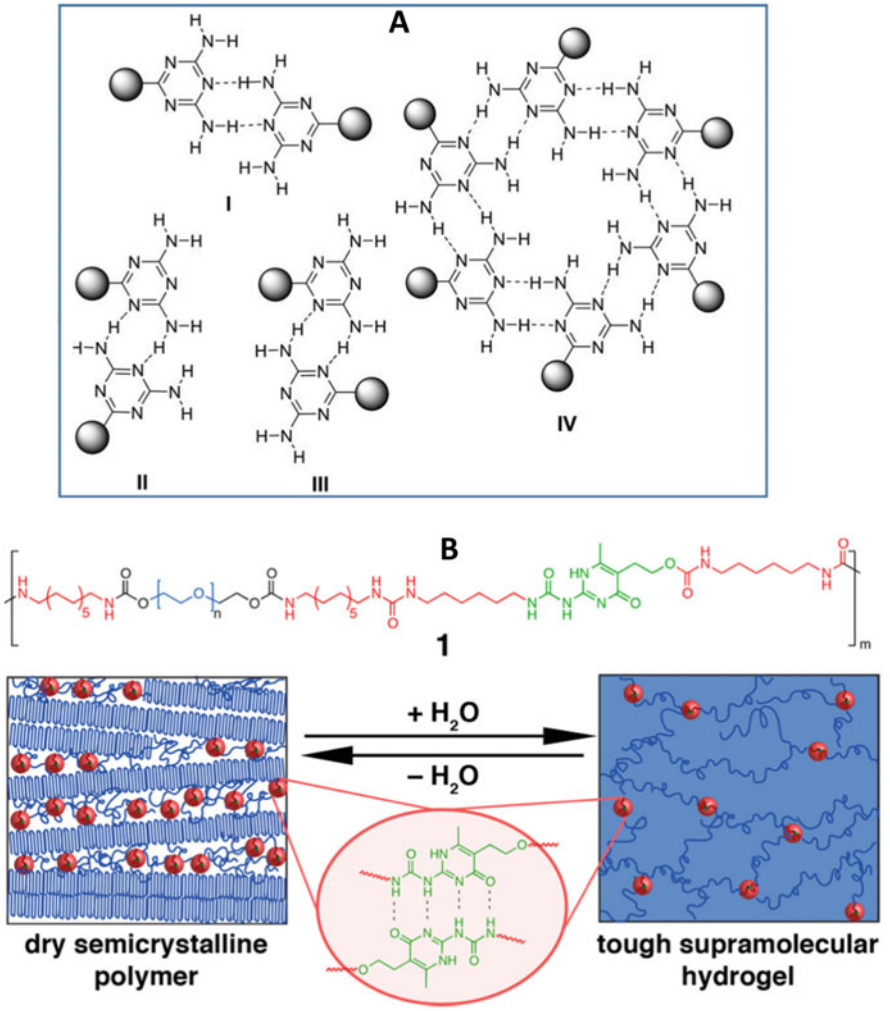

Fig. 3 (**a**) Structure of DAT groups and their H-bonding sites shown by the dashed lines. From [33] with permission from the Royal Society of Chemistry. (**b**) UPy unit in a segmented amphiphilic polymer chain (upper panel) and quadruple H-bonds between UPys forming semicrystalline polymer morphology in dry state and reversible transition to hydrogel after swelling in water (bottom panel). From [36] with permission from the American Chemical Society

introduction of hydrophobic segments into the hydrophilic chains protects the quadruple H-bonding between UPy units. Physical hydrogels with 80 wt% water and containing UPy units in the backbone of segmented amphiphilic polymers having hydrophilic poly(ethylene glycol) (PEG) sustain up to ~1 MPa stresses (Fig. 3b) [36]. Bulk images of the hydrogels show existence of UPy-UPy dimers serving as physical cross-links which are surrounded by segregated hydrophobic regions dispersed within the PEG matrix. H-bonded hydrogels via UPy units were

also fabricated by the micellar copolymerization of acrylamide and an amphiphilic cross-linker consisting of an acrylic head, alkyl spacer, and UPy group providing both hydrophobic associations and H-bonds [37]. To increase the solubility of the cross-linker in the micellar solution, salt was included into the reaction solution to induce the micellar growth [38]. However, weak hydrogels with a modulus of around 2 kPa could be obtained likely because of the weakening effect of surfactant molecules on the hydrophobic interactions [38, 39]. Physical hydrogels via both H-bonding and hydrophobic interactions were recently fabricated by free-radical copolymerization of UPy methacrylate, n-octadecyl acrylate (C18A), and acrylic acid [40]. The hydrophobic interactions between crystallizable alkyl side chains of C18A and the quadruple hydrogen bonds between UPy segments act as dual cross-links of the hydrogels. The hydrogels with a water content between 40 and 80 wt% exhibit a high tensile strength (up to 4.6 MPa) and elongation at break (680%). It was shown that the UPy units promote formation of alkyl crystals, while alkyl side chains stabilize UPy-UPy dimers [40].

Incorporation of hydrophobic groups into the hydrogel network has a significant effect on the strength of H-bonds and hence the mechanical performance of hydrogels consisting of H-bond acceptor and donor comonomer units. For instance, introduction of methyl motif to acrylic acid (AAc), that is, the use of methacrylic acid (MAAc) instead of AAc, significantly improves the mechanical performance of H-bonded hydrogels [41]. The hydrogel based on MAAc and 1-vinylimidazole containing 50–60 wt% water exhibits a Young's modulus up to 170 MPa, whereas it two orders of magnitude decreases when MAAc is replaced with AAc in the gel preparation [42, 43].

High-strength self-recovery hydrogels with a high Young's modulus (28 MPa), tensile strength (2 MPa), stretch at break (800%), and a good fatigue resistance were prepared by free-radical copolymerization of N,N-dimethylacrylamide (DMAA) and MAAc in aqueous solutions without a chemical cross-linker [41]. It was shown that the strong H-bond acceptor carbonyl group of DMAA and H-bond donor carboxylic group of MAAc form multiple H-bonds, leading to the formation of polymer-rich aggregates stabilized by the hydrophobic interactions of the α-methyl groups of MAAc units (Fig. 4). These aggregates serving as sacrificial cross-links ensure a high energy dissipation within the gel network. If MAAc segments in the hydrogel are replaced with AAc ones at the same concentration and water content, soft hydrogels with a fracture strength of less than 100 kPa could be obtained [41]. However, insolubility of DMAA/MAAc hydrogels in aqueous urea solutions reveals the existence of chemical cross-links in these self-recovery hydrogels likely due to the chain transfer reactions during copolymerization.

High-strength self-recovery H-bonded hydrogels were also prepared by simply heating aqueous solutions of acrylamide (AAm) and poly(N-vinylpyrrolidone) (PVP) at 56°C for 36 h without any chemical initiator or cross-linker (Fig. 5) [44]. The hydrogels with 60% water exhibit a high Young's modulus (84 MPa), tensile strength (1.2 MPa), and elongation at break (~3,000%). It was shown that AAm polymerization occurs by self-initiation at elevated temperature, whereas the presence of PVP provides formation of high-strength hydrogels. Insolubility of

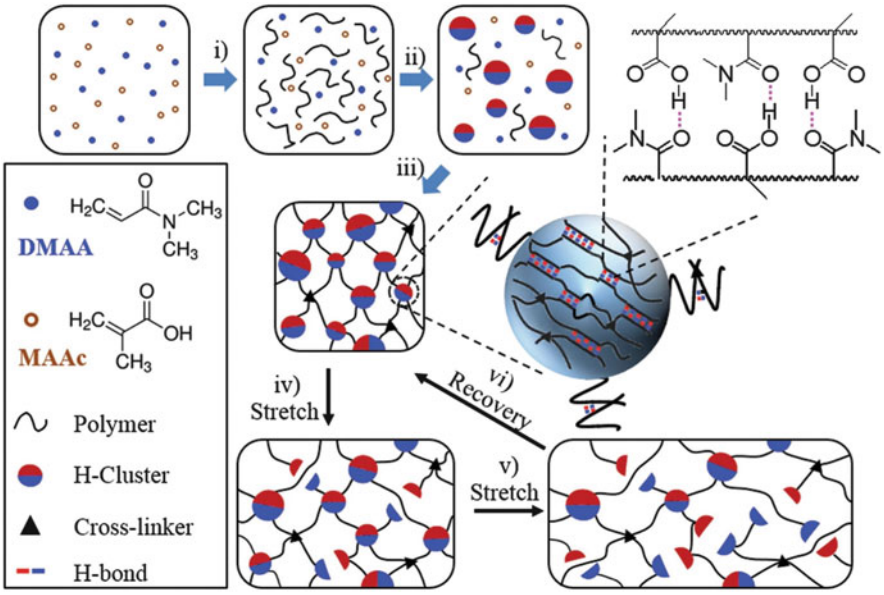

Fig. 4 Scheme illustrating formation of MAAc/DMAA hydrogels. Formation of oligomeric radicals (i), their phase separation due to multiple H-bonds to form polymer-rich clusters with trapped radicals (ii), and formation of a hydrogel containing clusters embedded into a polymer poor phase (iii). Stretching the hydrogel leads to fragmentation of weak (iv) and strong clusters (v) followed by complete recovery after unloading (vi). From [41] with permission from Wiley

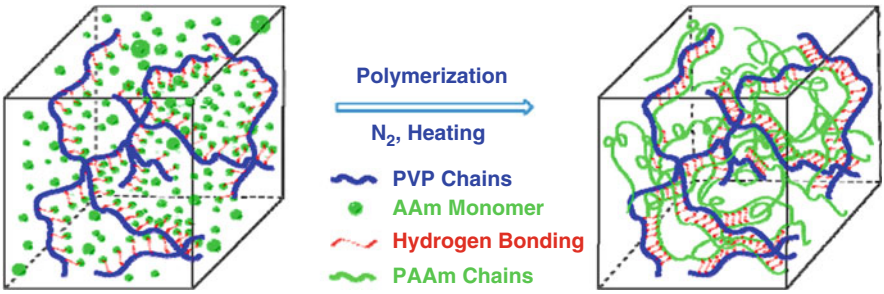

Fig. 5 Cartoon showing formation of PVP in situ PAAm hydrogels. From [44] with permission from the American Chemical Society

the hydrogels in water but their solubility in aqueous solutions of urea, a powerful H-bond-breaking reagent, reveal that they are purely formed via H-bonding interactions between the amide group of AAm and the pyrrolidone ring of PVP segments [44]. Interestingly, the copolymerization of AAm with the monomer of PVP, i.e., N-vinyl-2-pyrrolidone, instead of its homopolymerization in the presence of preexisting PVP under the same reaction condition leads to physical hydrogels with an order of magnitude lower tensile strength. This indicates that, as compared

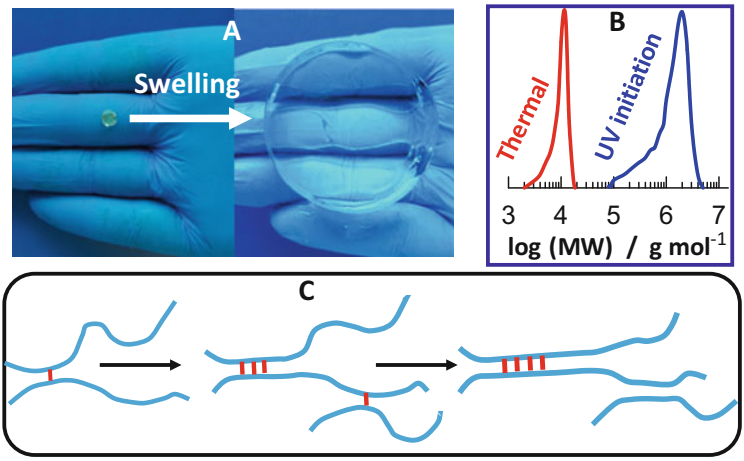

Fig. 6 (**a**) Images of a PAMPS hydrogel specimen formed at 60 wt% AMPS just after preparation and after equilibrium swelling in water. From [28] with permission from the American Chemical Society. (**b**) GPC curves of PAMPS primary chains obtained by solubilization of the hydrogels in an aqueous urea solution. The hydrogels were prepared by thermal and UV polymerizations at 50 wt% AMPS. (**c**) Cartoon presenting formation of multiple H-bonds (red lines) due to the proximity effect

to the preexisting PVP, in situ formed PVP produces much weaker H-bonds with the in situ formed PAAm chains. This finding was explained with the higher molecular weight of preexisting PVP than the in situ formed one, creating stronger cooperativity in H-bonding interactions due to the so-called proximity effect [45, 46]. Thus, once H-bonds are formed between two polymer molecules, their conformational freedom is restricted, facilitating formation of subsequent H-bonds, the extent of which increases with increasing number of segments in a polymer molecule. In addition, trapping effect of H-bonds may also increase the lifetime of chain entanglements leading to entanglement cross-links.

Increasing H-bond cooperativity with increasing molecular weight of primary chains was also observed for 2-acrylamido-2-methyl-1-propanesulfonic acid (AMPS) hydrogels, which are attracting increasing interest for the fabrication of superabsorbent materials [47]. Physical poly(AMPS) (PAMPS) hydrogels without any added chemical cross-linker and initiator were first prepared by Xing et al. using thermal polymerization of aqueous solutions of AMPS at 80°C [48]. Although PAMPS hydrogels exhibit a high stretchability (~2,500%) and self-healing efficiency, they are easily soluble in water indicating that the H-bond strength between the amino and carbonyl groups of AMPS segments is insufficient to withstand the osmotic pressure of AMPS counterions [48, 49]. Interestingly, AMPS polymerization under the same experimental condition except under UV light using a photoinitiator at room temperature produces water-insoluble PAMPS hydrogels exhibiting a degree of swelling of around 1,000 g g^{-1} (Fig. 6a) [28]. The hydrogels exhibit a Young's modulus of 30 kPa which is around threefold higher than those formed by thermal polymerization. PAMPS hydrogels formed by thermal and UV

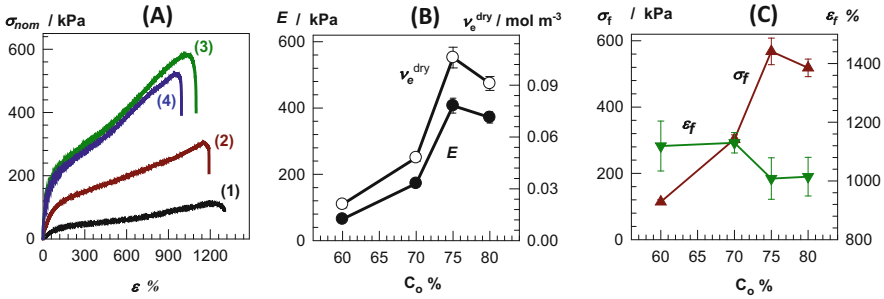

Fig. 7 (**a**) Nominal tensile stress (σ_{nom})-strain (ε) curves of AMPS/DMAA hydrogels formed at various monomer concentrations C_o and mole fractions x_{DMAA} of DMAA. For the curves labeled with 1, 2, 3, and 4, C_o and x_{DMAA} (in parenthesis) are 60 (0), 70 (0.46), 75 (0.62), and 80 wt% (0.74), respectively. (**b**, **c**) C_o dependences of the modulus E, cross-link density ν_e^{dry}, tensile strength σ_f, and elongation at break ε_f of the hydrogels. From [28] with permission from the American Chemical Society

polymerizations are easily soluble in aqueous solutions of urea indicating that they both form by H-bonding interactions. The main difference between two hydrogels was the molecular weight of the primary chains, i.e., 8.3×10^3 vs 7.5×10^5 g mol^{-1} for those formed via thermal and UV polymerization, respectively (Fig. 6b) [28]. This finding also highlights the importance of the proximity effect in the H-bond connectivity [45, 46]. As schematically illustrated in Fig. 6c, formation of a H-bond between two polymer chains facilitates formation of additional H-bonds in the vicinity because of the restricted conformation of chain segments in this volume element. As a consequence, increasing chain length also increases the number of H-bonds between polymers in H-bonded hydrogels.

Poly(DMAA) (PDMAA) is a versatile hydrophilic biocompatible polymer exhibiting associativity due to its dimethyl groups [50–54]. Although the segments of PDMAA with their dimethyl amino groups cannot form H-bonds between each other, they have an enhanced H-bond acceptor capability through their carbonyl groups via σ-donation effect of the methyl groups. Therefore, DMAA increases the H-bonding cooperativity in hydrogels when it is copolymerized with H-donor monomers. For example, UV polymerization of aqueous solutions of AMPS and DMAA in the absence of a chemical cross-linker leads to high-strength physical hydrogels with water contents between 30 and 40% [28]. Quantum mechanical calculations indeed reveal that the H-bond strength between AMPS/DMAA copolymers is much stronger than that between AMPS polymers [28]. AMPS/DMAA hydrogels in as-prepared state have a high Young's modulus (up to 0.41 MPa), tensile strength (~0.57 MPa), stretch at break (~1,000%), and self-healing efficiency (100%) and absorb a large amount of water at swelling equilibrium (up to ~1,700 g g^{-1}) (Fig. 7). The effective cross-link density ν_e^{dry} of the hydrogels significantly increases as the DMAA content of the network chains increases indicating formation of increased number of strong H-bonds serving as cross-links [28].

DNA existing in all living cells acts as the carrier of genetic information in their base sequences. Previous work shows that the entrapment of double-stranded (ds)-DNA within a clay hydrogel network enhances its bioresponsivity and degradation stability [55, 56]. For example, ds-DNA is easily digested by the DNase, whereas it is efficiently protected from DNase digestion and conserves its biological function in a clay environment [56]. The protection of ds-DNA provided by clay hydrogel is possibly important in the life's origin and sustainability on the earth. Haraguchi showed that Laponite clay nanoparticles in water serve as a multifunctional cross-linker during the polymerization of hydrophilic monomers such as N-isopropylacrylamide (NIPAM) or DMAA leading to the formation of highly stretchable and tough hydrogels [57–63]. Recently, self-healable DNA/clay nanocomposite hydrogels were fabricated by free-radical polymerization of DMAA in aqueous solutions of ds-DNA (~2,000 bp, molecular weight $= 1.3 \times 10^6$ g mol^{-1}) and Laponite [15]. From the cyclic mechanical tests, the intermolecular bond strength in the hydrogels was estimated as 2.7 ± 0.2 kJ mol^{-1} which is close to that of H-bonds. It was shown that Laponite nanoparticles contribute to the elastic behavior of DNA/clay hydrogels, whereas their DNA component promotes the energy dissipation under stress [15]. This is due to the repulsive interactions between equally charged DNA and surfaces of disk-like Laponite nanoparticles in water [57, 64, 65], preventing H-bonding between each other so that DNA can move freely between the nanoparticles contributing to the energy dissipation.

Although DNA/clay hydrogels have a low modulus and tensile strength in the kPa range, they are highly stretchable (up to 1,500%) and display the characteristics of ds-DNA such as its thermally induced denaturation and renaturation behavior [15]. To highlight this feature, the hydrogels were prepared in the presence of ethidium bromide (EtBr), which is known to intercalate between ds-DNA base pairs leading to a higher fluorescence intensity as compared to the single-stranded (ss)-DNA [66, 67]. Figure 8a shows fluorescence spectra of EtBr in a DNA/clay hydrogel during a thermal cycle between 25 and 90°C, while the inset shows temperature dependence of EtBr emission intensity at 600 nm [15]. With increasing temperature, labeled by 1 to 5 in the figure, the peak intensity decreases, whereas it again increases after cooling back to 25°C, labeled by 6, revealing denaturation-renaturation of ds-DNA within the gel network. The optical images of a gel sample under UV light also visualize this conformational transition between ds- and ss-DNA (Fig. 8b); the yellow-orange color of the gel becomes lighter with increasing temperature up to 90°C but cooling back to 25°C recovers its initial color. Thus, ds-DNA in the hydrogels dissociate into single strands when heated above its melting temperature T_m, whereas the double-stranded conformation is recovered after cooling back below T_m.

DNA/clay hydrogels also display an interesting healing mechanism based on the denaturation and renaturation behavior of ds-DNA encapsulated within the hydrogel [15]. When the cut regions of a hydrogel specimen are heated above T_m of ds-DNA and then pushed together following by cooling below T_m, the hydrogel exhibits a high healing efficiency. For instance, heating a damaged hydrogel specimen

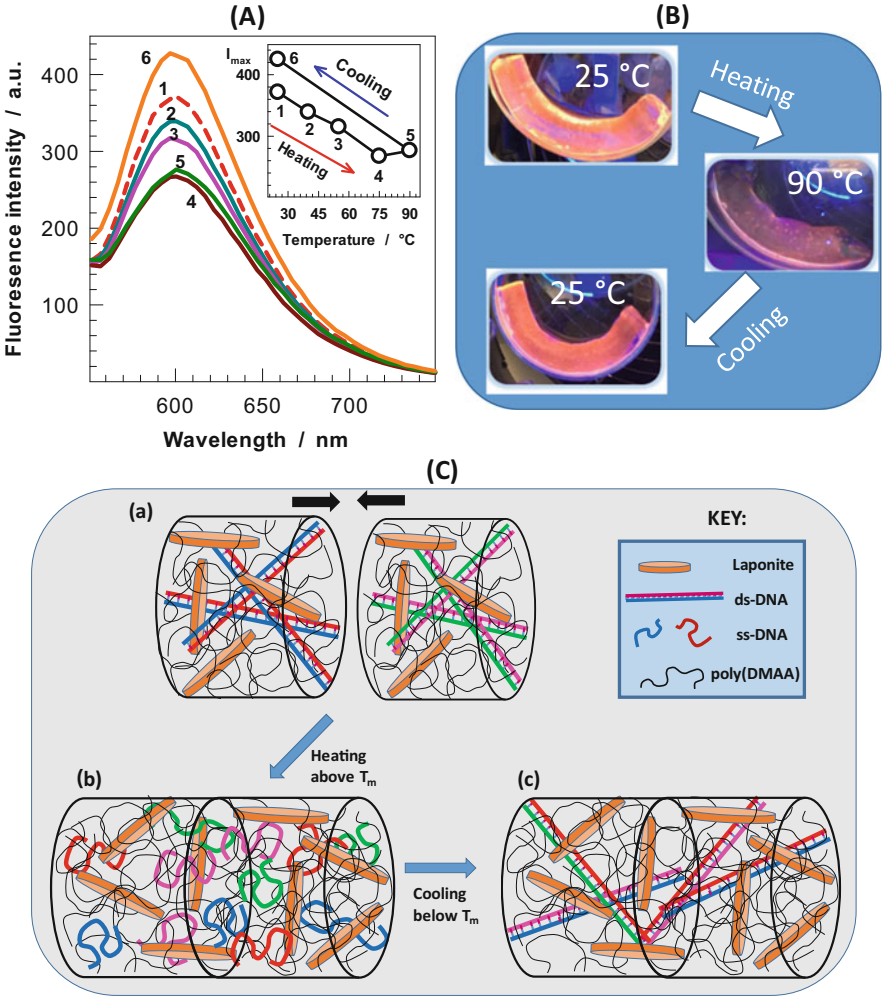

Fig. 8 (**a**) Effect of temperature on the fluorescence spectra of EtBr in a DNA/clay hydrogel. For the spectra labeled by 1–6, the temperatures are 25, 40, 55, 75, 90°C, and after cooling back to 25°C, respectively. The inset shows temperature dependence of EtBr emission intensity at 600 nm. Laponite = 5 w/v %. DNA = 4 w/v %. (**b**) Optical images of a EtBr-containing DNA/clay hydrogel sample under UV light at 25 and 90°C and after cooling back to 25°C. (**c**) Schematic presentation of the cut area of a DNA/clay hydrogel (**a**), after bringing the cut surfaces together at $T > T_m$ (**b**), and after cooling below T_m of ds-DNA (**c**). From [15] with permission from the American Chemical Society

containing 5 w/v % Laponite and 4 w/v % DNA at 90°C for 30 min results in an almost complete healing with respect to the stretch ratio. Because denaturation of the semiflexible ds-DNA at 90°C produces flexible ss-DNA strands with much higher mobility [66, 68, 69], the single strands at the cut region can easily move between the

surfaces so that, after cooling below T_m, ds-DNA bridges formed between the surfaces provide healing of the hydrogels (Fig. 8c) [15].

Self-recovery hydrogels via both dipole-dipole and H-bonding interactions were fabricated by copolymerization of the dipole acrylonitrile, H-bonding acrylamide (AAm), anionic AMPS, and a hydrophilic cross-linker in DMSO as the solvent, which was replaced with water after the reaction [70]. It was shown that the amount of ionic AMPS segments in the gel network regulates the water content between 32 and 98%, whereas the collaborative effect of H-bonding and dipole-dipole interactions leads to mechanically robust hydrogels with a tensile strength and elongation at break up to ~8 MPa and 700%, respectively. Self-recovery double-network hydrogels based on poly(acrylic acid) and poly(N-isopropyl acrylamide) were prepared by both chemical cross-links and H-bonds [71]. Young's modulus of the hydrogels is around 226 MPa at room temperature, but it significantly decreases at elevated temperature indicating that the cooperative H-bonds mainly determine the cross-link density of the hydrogels.

Hydrogels via both electrostatic and H-bonding interactions were prepared by mixing of a solution of the cationic polyelectrolytes poly(diallyldimethylammonium chloride) and branched poly(ethylenimine) (PEI) with another solution of anionic polyelectrolytes poly(sodium 4-styrenesulfonate) and poly(acrylic acid), followed by molding, drying, and rehydration [72]. The hydrogels with 42% water content having oppositely charged ionic groups and H-bond forming sites exhibit a modulus, tensile strength, and elongation at break of 0.4 MPa, 1 MPa, and 2,400%, respectively, and a complete healing efficiency after immersing in water at room temperature for 14 h. Mixing of aqueous solutions or hydrogels of ionic polymers with oppositely charged ions was also utilized to create hydrogels via reversible ionic bonds enabling an efficient energy dissipation [73, 74]. Immersion of a loosely cross-linked poly(acrylamide-co-acrylic acid) hydrogel in aqueous $FeCl_3$ solution to form the physical cross-links followed by washing with water to remove the excess ions leads to self-recoverable hydrogels with a high modulus (3 MPa), tensile strength (6 MPa), and 500% elongation at break [75]. Ionic nanocomposite self-healing hydrogels were prepared from acrylic acid (AAc), vinyl hybrid silica nanoparticles (VSNPs), and Fe^{3+} ions by free-radical polymerization [76]. Physical cross-links between PAAc chains and Fe^{3+} ions lead to nanocomposite physical hydrogels with a tensile strength and elongation at break of 0.9 MPa and 2,300%, respectively, exhibiting self-healing ability at elevated temperature recovering 1,800% elongation at break and 0.56 MPa tensile strength [76]. Self-healing hydrogels were also prepared using Fe^{3+} ions and carboxylated cellulose nanofibrils (CNFs) as physical cross-linkers [77]. Carboxylated CNFs form H-bonds with poly (acrylic acid) (PAAc) chains, whereas Fe^{3+} forms ionic bonds with the carboxylic groups of both PAAc and carboxylated CNFs. The hydrogels exhibit a relatively high tensile strength, elongation at break, and healing efficiency of 4 MPa, 180%, and 87%, respectively [77]. Hydrogels based on cationic polyacrylamides reinforced with graphene oxide (GO) exhibit an efficient energy dissipation under stress due to the H-bonding and ionic interactions between AAm-GO and GO-cationic segments, respectively [78]. Both the amount of GO and the copolymer composition are the

main factors determining the mechanical performance and self-healing efficiency of the hydrogels. The hydrogels with a tensile strength of ~0.5 MPa exhibit a self-healing efficiency of around 90% with respect to the tensile strength, elongation at break, and toughness. Elastin-like polypeptides consisting of a long hydrophobic block with hydrophilic ends also form self-healing hydrogels via hydrophobic and ionic interactions [79]. Heating polypeptide solution triggers the self-assembly of polypeptides to form micelles which were then cross-linked using zinc ions via metal coordination. At 10% polypeptide concentration, the hydrogels exhibit a storage modulus of ~1 MPa and an effective self-healing behavior within minutes [79].

3 Hydrophobic Interactions

Segregation tendency of water-fearing (hydrophobic) molecules and water, which is called hydrophobic interactions, is important in many self-assembly processes such as formation of micelles, protein folding, and molecular recognition [80]. The driving force for the hydrophobic interactions arises to reduce the hydrophobic moieties of their exposure to water leading to hydrophobic associations and crystalline regions. Fu et al. used the amphiphilic triblock copolymer F127 for preparing hydrophobically cross-linked micellar hydrogels [81], which are reviewed in this volume [82]. Weiss et al. used fluoroacrylate monomers in the preparation of hydrophobically modified fluorocarbon-based hydrogels [83]. The strong hydrophobic interactions between fluoroacrylate segments lead to core-shell nanodomains within the hydrogels providing a MPa level modulus, as also detailed in this volume [84]. In the following, we first discuss the studies conducted on self-healing hydrocarbon-based hydrogels formed by hydrophobic associations exhibiting a modulus in the kPa range and a high stretchability. In the second section, the order-to-disorder transition from association to alkyl crystals and formation of high-strength self-healing semicrystalline hydrogels with a modulus and tensile strength in the range of MPa are discussed.

3.1 Hydrophobically Modified Associative Hydrogels

Creton and co-workers were the first to report that hydrophobic modification of chemically cross-linked polyelectrolyte hydrogels creates variable dissipative properties at almost identical cross-link densities [85]. They showed that the incorporation of hydrophobic side groups into polyelectrolyte hydrogels significantly increases their loss moduli and hence generates energy dissipation because of the formation of hydrophobic associations serving as reversible cross-links. However, a complicated three-step synthetic approach was used for the synthesis of such hybrid cross-linked hydrogels due to the solubility mismatches between hydrophilic and hydrophobic monomers [85]. The micellar polymerization technique is a simple and

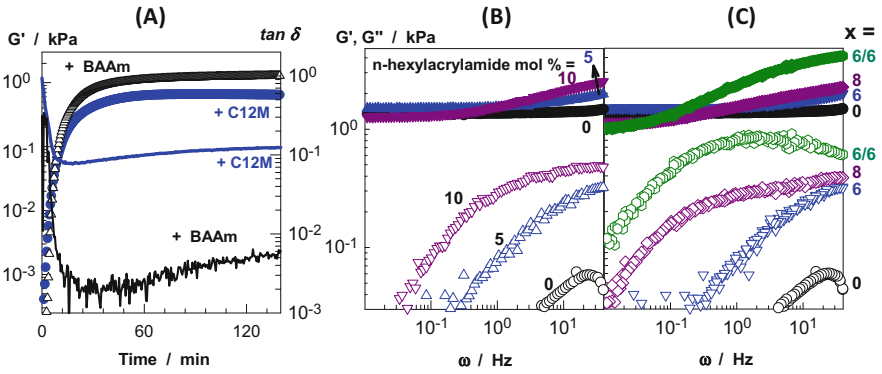

Fig. 9 (**a**) Storage modulus G' (symbols) and the loss factor tan δ (lines) during the micellar polymerization of AAm in the presence of dodecyl methacrylate C12M or BAAm, each 1 mol%, in aqueous 7 w/v % SDS solution. $\omega = 6.28$ rad/s. $\gamma_o = 0.01$. From [96] with permission from Elsevier. (**b**, **c**) Frequency dependences of G' (filled symbols) and loss modulus G'' (open symbols) of chemically cross-linked PAAm hydrogels containing N-alkylacrylamide segments. $\gamma_o = 0.01$. BAAm = 1.25 mol%. (**b**) N-Hexylacrylamide concentration = 0 (●, □), 5 (▲, Δ), and 10 mol% (▼, ∇). (**c**) Hydrophobic monomer = 5 mol%. The alkyl chain length x of the hydrophobes is indicated. From [95] with permission from Elsevier

versatile alternative for copolymerizing water-soluble and water-insoluble monomers in aqueous solutions [86–90]. By this technique, hydrophobic monomers solubilized in a micellar solution are copolymerized with hydrophilic monomers by free-radical mechanism. Because of the locally high concentration of hydrophobic monomers within the surfactant micelles, copolymer chains containing blocks of hydrophobes are obtained providing stronger hydrophobic interactions as compared to the random copolymers formed by solution or bulk polymerizations [91]. The length of hydrophobic blocks and the number of blocks per copolymer chains can easily be adjusted by the concentrations of surfactant and hydrophobic monomer. Candau et al. showed significant effects of the number and length of hydrophobic blocks on the zero-shear viscosity of semi-dilute solutions of hydrophobically modified polyacrylamides [86–90, 92–94]. However, physically or hybrid, i.e., chemically and physically, cross-linked analogs of these polymers in their as-prepared or swollen states in water as well as their mechanical and viscoelastic properties draw attention only in the past years [95–100].

Figure 9a illustrates a typical example comparing the effect of a hydrophobic monomer, dodecyl methacrylate (C12M), as a physical cross-linker with the classical chemical cross-linker N,N′-methylenebis(acrylamide) (BAAm) on the hydrogel formation [96]. Here, the storage modulus G' (symbols) and the loss factor tan δ (lines) of the reaction systems are shown as a function of the reaction time during the micellar polymerization of acrylamide (AAm) with C12M or BAAm, each 1 mol% (with respect to AAm) in an aqueous sodium dodecyl sulfate (SDS) solution. Incorporation of C12M segments into the PAAm chains produces a hydrogel with one order of magnitude higher tan δ than that obtained using BAAm cross-linker

during which the storage modulus G' only slightly decreases. This indicates the dynamic nature of the cross-link regions in C12M-containing hydrogels as compared to the chemically cross-linked ones because of the reversible dissociation and reassociation of the dodecyl side chains. Figure 9b shows frequency dependences of G' (filled symbols) and G'' (open symbols) of hybrid cross-linked PAAm hydrogels containing 0–10% n-hexylacrylamide and 1.25 mol% BAAm [95]. At low frequencies, i.e., at long experimental time scales, they all exhibit similar mechanical spectra, i.e., G' is frequency independent and G'' is more than an order of magnitude smaller than G', as typical for strong gels. However, at the high frequency range, G'' significantly increases both with the frequency and the hydrophobe content reflecting energy dissipation due to the reversible nature of hydrophobic associations that are captured at short experimental time scales. The length x of the alkyl side chain of n-alkylacrylamides has a similar effect on the properties of PAAm hydrogels (Fig. 9c) [95]. Increasing the side chain length x at a fixed hydrophobe content shortens the width of G' plateau, i.e., G'' and G' start to increase at lower frequencies. This reveals increasing lifetime of hydrophobic associations with increasing alkyl side chain length of the hydrophobic monomers. Thus, long-lived hydrophobic associations and hence mechanically strong hydrogels could be generated using long alkyl side chains. However, (meth)acrylates larger than 12 carbon atoms at their side chains such as n-octadecyl acrylate (C18A) or docosyl acrylate (C22A) could not be solubilized in monomeric, spherical surfactant micelles due to their larger sizes as compared to the micelles, hindering their micellar copolymerization with hydrophilic monomers.

Worm-like micelles (WLMs) formed by self-assembly of surfactant micelles exhibit interesting rheological properties and a significant solubilization power for hydrophobes, and thus, they are able to form nano-sized oil depots dispersed in water [14, 38, 91, 101–103]. A simple way to produce WLMs is the addition of salts such as NaCl to the aqueous solutions of ionic surfactants which weakens the electrostatic repulsion between the monomeric micelles and hence promotes their growth to form "polymer-like" micelles. As shown in Fig. 10a, addition of 1 M NaCl in an aqueous solution of 7.6 w/v % SDS increases the zero-shear viscosity η_o by more than two orders of magnitude, and simultaneously, the hydrodynamic correlation length ξ_H increases from below 1 to 20 nm due to the micellar growth [102]. Formation of WLMs provides solubilization of large hydrophobes in SDS-NaCl solutions. For instance, C18A monomer, which is insoluble in aqueous SDS solutions, could be solubilized up to 15 w/v % in WLMs formed by the addition of 1.5 M NaCl into 22 w/v % aqueous SDS at 55°C (Fig. 10b) [91]. Interestingly, after solubilization of the hydrophobes in WLMs, both the zero-shear viscosity and hydrodynamic correlation length ξ_H reduce to a low level (Fig. 10c). SANS and cryo-EM measurements revealed that WLMs undergo a conformational transition from cylindrical to spherical shape after addition of hydrophobes, which is responsible for the decrease in the zero-shear viscosities [14, 102]. The accumulation of the hydrophobic monomers inside the core of the micelles creating a curvature on the micelle surface seems to be responsible for the conformational change in SDS micelles. Moreover, micellar copolymerization of hydrophilic monomers with a large amount of hydrophobic

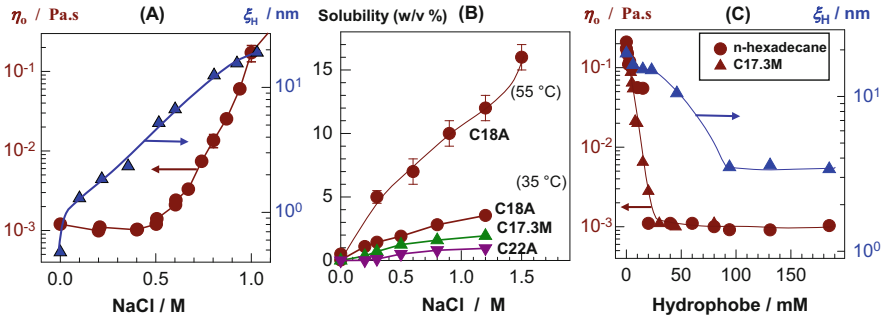

Fig. 10 (**a**) NaCl concentration dependences of the zero-shear viscosity η_o (circles) and hydrodynamic correlation length ξ_H (triangles) of 7.6 w/v % SDS solution at 35°C. From [102] with permission from the American Chemical Society. (**b**) NaCl concentration dependence of the solubility of C17.3M, C18A, and C22A in aqueous SDS solutions. The data are for 7 and 22 w/v % SDS at 35 and 55°C, respectively. (**c**) Variations of η_o and ξ_H of 7.6 w/v % SDS – 1 M NaCl solution at 35°C with the addition of n-hexadecane and C17.3 M monomer. From [102] with permission from the American Chemical Society

monomer such as C18A or stearyl methacrylate C17.3M (a mixture of n-octadecyl- and n-hexadecyl methacrylates with an average alkyl side chain length of 17.3 carbons) solubilized in WLMs results in hydrogels with strong hydrophobic interactions providing transformation of hydrophobic associations into alkyl crystals as will be discussed in the next section.

Depending on the presence of surfactant micelles, hydrophobically modified hydrogels undergo drastic changes in their viscoelastic and self-healing properties [38]. Those with surfactant are mechanically weak with a few kPa modulus and exhibit autonomic self-healing behavior, whereas without surfactant, the modulus increases to tens of kPa, but they have no more self-healing ability even at elevated temperatures. A typical example is the hydrogels synthesized by micellar polymerization of 10 w/v % AAm in the presence of 2 mol% C17.3M (with respect to AAm) in aqueous solutions of worm-like SDS micelles [104]. The corresponding SDS-free hydrogels were fabricated by extracting SDS from as-prepared hydrogels in an excess of water. It was shown that Young's modulus and compressive strength around five- and ninefold increase, respectively, while the stretch at break twofold decreases after extraction of SDS from the hydrogels [104]. This reveals a significant increase in the strength of hydrophobic interactions in the absence of surfactant molecules. Theoretical studies indeed indicate that surfactant molecules considerably affect the hydrophobic associations in the hydrogels [105]. It was shown that the sorption of surfactant molecules by hydrophobically modified hydrogels is noncooperative and they continuously incorporate within the existing hydrophobic aggregates to form mixed micelles, thereby decreasing the effective cross-link density of the hydrogel. Recent works show stiffening effect of SDS on hydrophobically modified physical hydrogels at a low SDS concentration which is due to the increased chain mobility facilitating formation of additional

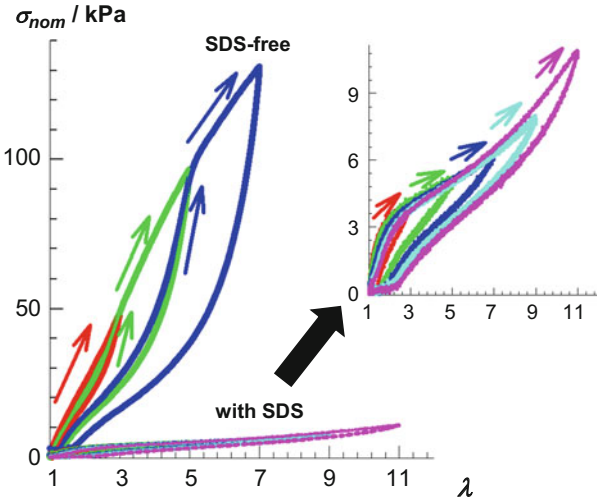

Fig. 11 Multistep tensile cyclic tests conducted on SDS-free and SDS-containing PAAm hydrogels with 2 mol% C17.3M. The inset is zoom-in to the data of hydrogel with SDS. From [104] with permission from Springer

supramolecular bonds [106, 107]. However, increasing SDS concentration in the hydrogel results in a gel-to-sol transition due to the dissolution of the mixed micelles.

Mechanical cyclic tests are a mean to compare the strength of hydrophobic interactions in the hydrogels. Figure 11 shows typical multistep tensile cycles conducted on PAAm hydrogels containing 2 mol% C17.3M with and without SDS where the inset is zoom-in to the data of the SDS-containing hydrogel [104]. The data are shown as the nominal stress (σ_{nom})-strain (λ) curves where λ is the stretch ratio. The tests were carried out by stepwise increasing the maximum strain with a wait time of 7 min between each cycle. For a given maximum strain λ, the mechanical hysteresis in SDS-free hydrogel is much larger than that of the corresponding SDS-containing one, indicating higher strength of hydrophobic associations in the former hydrogel. Moreover, as seen in the inset to Fig. 11, the hydrogel containing SDS undergoes reversible tensile cycles, i.e., each loading curve follows the path of the previous loading indicating healing of the damage during the wait time between cycles. In contrast, SDS-free hydrogel exhibits irreversible cycles each of which creates additional damage that cannot be healed during the wait time. Indeed, SDS-containing hydrogel has a complete self-healing efficiency, whereas SDS-free hydrogel has lack the ability to self-heal even after prolonged healed times at elevated temperature or by treating the cut regions with 7 w/v % SDS solution up to 12 days [104]. Healing in SDS-free hydrogels could only be induced by the treatment of the cut region with an aqueous solution of worm-like SDS micelles. This reveals that WLMs are able to solubilize the hydrophobic domains at the cut surfaces so that they merge together by reformation of the physical cross-links.

To highlight the effect of the hydrophilic monomer type on the mechanical properties of hydrophobically modified hydrogels, micellar copolymerizations of

hydrophilic AAm, NIPAM, and DMAA monomers were conducted with 2 mol% C17.3M hydrophobe in aqueous solutions of WLMs [38, 108, 109]. The surfactant-containing hydrogels prepared using DMAA exhibit the highest stretchability, 4,200 ± 400%, as compared to those formed using AAm and NIPAM that can sustain stretches up to 2,000%, which was attributed to the associative behavior of DMAA segments (Fig. 12a). Hydrophobically modified PDMAA hydrogels

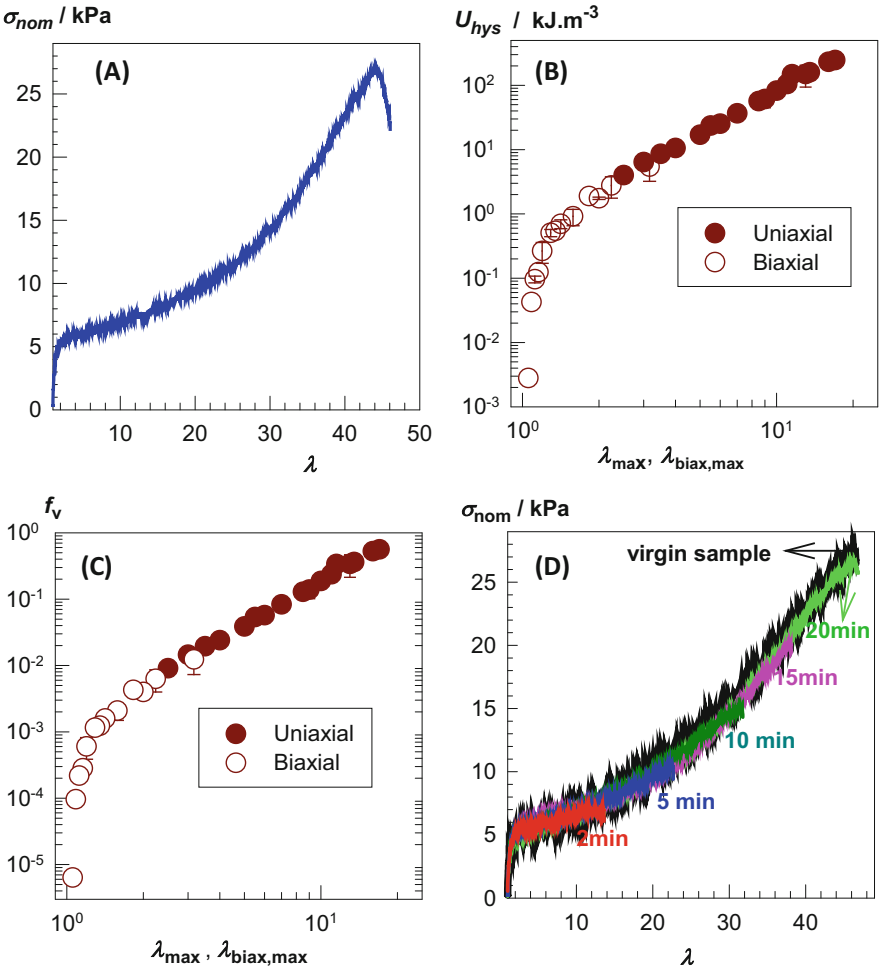

Fig. 12 Large strain and self-healing behaviors of a PDMAA hydrogel with 2 mol% C17.3M. The hydrogel was prepared at 10 w/v % DMAA concentration in an aqueous 0.5 M NaCl solution containing 7 w/v % SDS. (**a**) Typical tensile stress-strain curve of a hydrogel specimen at a strain rate of 1.56×10^{-2} s^{-1}. (**b**, **c**) Hysteresis energy U_{hys} (**b**) and the fraction of reversibly broken intermolecular bonds, f_v, (**c**) of the hydrogel calculated from successive tensile (filled circles) and compression cycles (open symbols) plotted against the maximum stretch ratio (λ_{max} and $\lambda_{biax,max}$). The waiting time between cycles is 7 min. (**d**) Tensile stress-strain curves of virgin and healed hydrogels at various healing times at 24°C as indicated. From [108] with permission from Elsevier

subjected to mechanical cycles exhibit hysteresis whose extent continuously increases with the maximum strain indicating breakage of intermolecular bonds of varying strength [108]. However, if the cyclic tests are repeated several times with a wait time of 7 min between cycles, all the cycles overlap well for a given maximum strain, which is an indication of reformation of the broken bonds during the wait time.

Figure 12b shows maximum strain dependence of the hysteresis energy U_{hys}, calculated as the area surrounded by the loading and unloading curves, of successive tensile (filled circles) and compressive cycles (open circles). Because uniaxial compression ratio equals to the reciprocal of the square root of the biaxial extension ratio, U_{hys} data could be plotted against a common abscissa, namely, the uniaxial (λ_{max}) and biaxial maximum stretch ratios ($\lambda_{biax,max}$). Over the whole range of maximum strain, the hysteresis energies U_{hys} fall into a single curve revealing that U_{hys} is independent on the type of strain, and it only depends on the value of the maximum strain. Calculation of the fraction f_v of reversibly broken bonds during the mechanical cycles reveals that more than half of the intermolecular bonds, i.e., up to at least $f_v = 0.56$, can be broken reversibly at a stretch ratio of around 20 (Fig. 12c) [108]. This is a sign of a high self-healing efficiency of PDMAA hydrogels without any external stimuli. Indeed, a complete healing in these hydrogels was achieved by holding their cut surfaces together at 24°C for 20 min (Fig. 12d) [108].

The mechanism of autonomic self-healing in surfactant-containing hydrogels was recently investigated by scanning force microscopy (SFM) measurements [102]. For this purpose, the surface of a hydrophobically modified PAAm hydrogel containing 2 mol% C17.3M was first cut with the SFM tip to create trenches of 20–40 nm in depth and protrusions of around 10 mm in height. Figure 13A shows topographic images (left panel) and cross sections of the gel surface (right panel) just after cutting (a), a few seconds after cutting (b), and after a wait time of 75 min (c). Interestingly, a terraced topography was observed for both protrusions and trenches with a step height between 3.8 and 5.0 nm, or multiples thereof, as indicated by the horizontal dotted lines in Fig. 13A. XRD measurements revealed that the smallest step height is close to the d spacing of the hydrogel (3.9 nm) [102]. This indicates the existence of layered hydrophobic nanodomains in the hydrophobically modified hydrogels as observed in comb-like polymers with alkyl side chains [110] and fluorocarbon-based hydrogels [83, 84]. Moreover, immediately after damaging, both the trenches and protrusions on the gel surface transform into rounded shapes without affecting their depth and height, respectively (a to b in Fig. 13A). In contrast to the fast reshaping process in the damaged area, the healing process, that is, the size reduction of the holes and islands on the hydrogel surface, and their disappearance require a relatively long time (b to c in Fig. 13A). Thus, healing of the gel surface occurs in two steps, namely, a fast reshaping of the damaged area into circular forms without healing followed by slow size reduction of this area and finally complete healing to recover the virgin surface [102]. The first step was attributed to the strong attractive interactions between the alkyl side chains of hydrophobic units locating in close

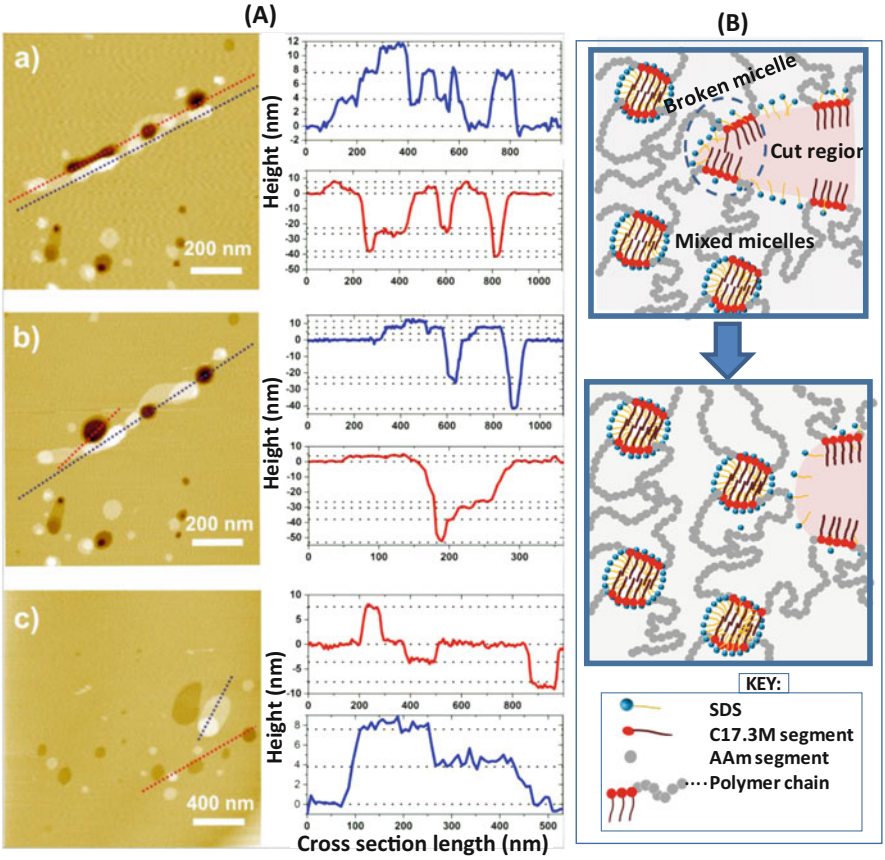

Fig. 13 (**A**) Topographic SFM images (left panel) and cross sections of the surface (right panel) of a PAAm hydrogel specimen with 2 mol% C17.3M. The images were taken just after cutting (**a**), right after the first image (**b**), and after a wait time of 75 min at 35°C and 87% relative humidity (**c**). The red and blue dotted lines across the trenches and protrusions on the images, respectively, show their cross sections at the right panel in respective colors. The dotted lines on the surface cross sections indicate steps of 3.8 nm or multiples thereof. Color scale = 50 nm (from black to white). (**B**) Schematic illustration of fast reshaping process of the trenches and protrusions on the gel surface into circular shapes due to the attractive interactions between hydrophobic C17.3M segments locating at the edge of a damaged micelle. From [102] with permission from the American Chemical Society

vicinity to each other, i.e., at the edge of the trenches, leading to the formation of round holes, as seen schematically in Fig. 13B. Because the consumption of the islands by the round holes and their disappearance require interlayer mobility of mixed micelles which is slow as compared to their mobility along the layers, the second step needs much longer times than the first one [102].

3.2 Mechanically Strong Hydrophobically Modified Hydrogels

Hydrogels formed in the presence of a small amount of a hydrophobic monomer via micellar polymerization discussed in the previous section have a high self-healing efficiency, but they exhibit an insufficient mechanical performance for load-bearing applications. Although their mechanical strength could be improved by incorporation of hydrophobic acrylates instead of the corresponding methacrylates into the hydrophilic polymer backbone, or by increasing the length of alkyl side chain of the hydrophobic monomers from 12 to 22 carbon atoms, the tensile strength only slightly increases from 20 to 65 kPa after these modifications [101]. Chen et al. conducted the micellar copolymerization of AAm and C18A by the addition of 1-pentanol as a cosurfactant of SDS solubilizing the hydrophobe in the micellar solution [111]. After γ-radiation induced polymerization without any initiator, they produced a hydrogel sustaining kPa level compressive stresses. However, swelling of this hydrogel in a second aqueous AAm-BAAm solution followed by polymerization leads to a self-recovery double-network PAAm hydrogel exhibiting a compressive strength of 2.8 MPa under 90% compression [111]. Micellar polymerization reactions conducted using a polymerizable (acrylated) cationic surfactant in the absence of free surfactants or reducing surfactant content using amphiphilic hydrophobic monomers lead to hydrogels with tensile strength up to ~300 kPa but with a low self-healing efficiency [112, 113]. Micellar polymerization of AAm and 2 mol% C17.3M in aqueous mixtures of cationic and anionic surfactants produces PAAm hydrogels with a high stretchability (1,800–5,000%) and complete self-healing efficiency but a low mechanical strength [114]. Thomas et al. prepared hydrophilic-hydrophobic hydrogels based on polyvinyl alcohol and poly(ethylene-co-vinyl alcohol) with 15–25% water content that exhibit good compressive properties with a modulus of around 20 MPa [115]. Moreover, creating hybrid cross-linked hydrophobically modified hydrogels by incorporation of chemical cross-links also provides some improvement in the compressive mechanical properties without affecting much their self-healing behavior, but they are brittle in tension [116]. Considering the load-bearing tissues such as cartilages, tendons, and ligaments containing 60–75% water and exhibiting a modulus and tensile strength in the range of MPa, one needs to improve the tensile mechanical performances of hydrophobically modified self-healing hydrogels to the MPa level. In the following subsections, two attempts will be discussed for fabrication of high-strength hydrophobically modified hydrogels with a high self-healing efficiency.

3.2.1 Hydrophobically Modified Polyelectrolyte Hydrogels with Oppositely Charged Surfactants

One attempt in this direction was to use oppositely charged surfactants in the preparation of hydrophobically modified polyelectrolyte hydrogels by micellar

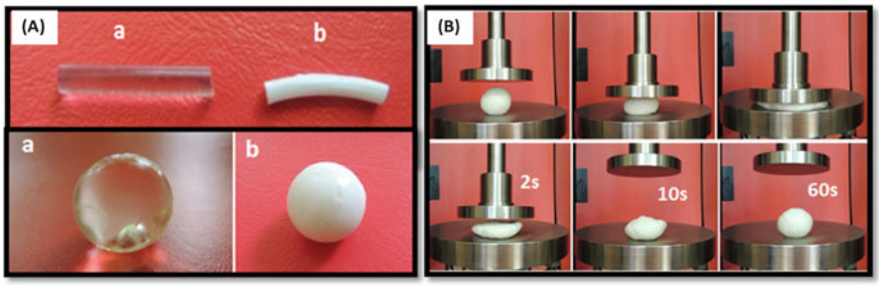

Fig. 14 (**A**) Images of two PAAc hydrogel specimens in as-prepared (**a**) and equilibrium swollen states in water (**b**). (**B**) Images of a spherical swollen PAAc hydrogel during loading (upper row) and 2, 10, and 60 s after unloading (bottom row). C_o = 20 w/v%. β_o = 1/8. From [117] with permission from the American Chemical Society

polymerization [117]. The interactions between polyelectrolytes and oppositely charged surfactants in an aqueous solution such as poly(acrylic acid) (PAAc) and cetyltrimethylammonium bromide (CTAB) have been investigated in detail during the past two decades [118–125]. It was shown that, at a high ionization degree of PAAc, electrostatic interactions determine the complex formation between PAAc and CTAB, whereas hydrophobic interactions start to dominate when the ionization is suppressed by decreasing the pH of the solution [118, 121]. Moreover, PAAc-CTAB interactions become stronger when a small amount of a hydrophobic segment carrying alkyl side chain is incorporated into the PAAc backbone because of the formation of mixed micelles composed of CTAB and alkyl side chains of hydrophobically modified PAAc [126, 127].

High-strength self-healing PAAc hydrogels were recently fabricated by micellar copolymerization of AAc and 2 mol% C17.3M in aqueous solutions of worm-like CTAB micelles [117]. It was found that PAAc-CTAB complexes in the hydrogel start to form after immersion in water, as visualized by its appearance changes from transparent to opaque (Fig. 14A). The late complexation between PAAc and CTAB within the hydrogel network is due to the low pH (1.5) of as-prepared hydrogels, while the pH increases to 6.7 after immersing in water, providing ionization of AAc segments and hence their complex formation with the cetyltrimethylammonium (CT) ions. Simultaneously, both G' and G'' increase by one order of magnitude, while the loss factor tan δ *r*emains above 0.1 revealing that the viscous character of the hydrogels is preserved in their swollen state [117]. This behavior is in contrast to the hydrophobically modified nonionic hydrogels prepared via micellar polymerization as discussed in the previous section. The viscoelastic nature of water-swollen PAAc hydrogels is presented in the images of Fig. 14B showing compression of a spherical PAAc hydrogel under load and complete recovery of the original shape within 1 min after unloading.

It was shown that the as-prepared hydrogels have weak physical cross-links consisting of mixed C17.3M and CTAB micelles [117], which are similar to those existing in SDS-containing nonionic hydrogels. However, after swelling equilibrium, i.e., after ionization of PAAc chains, a second type of much stronger

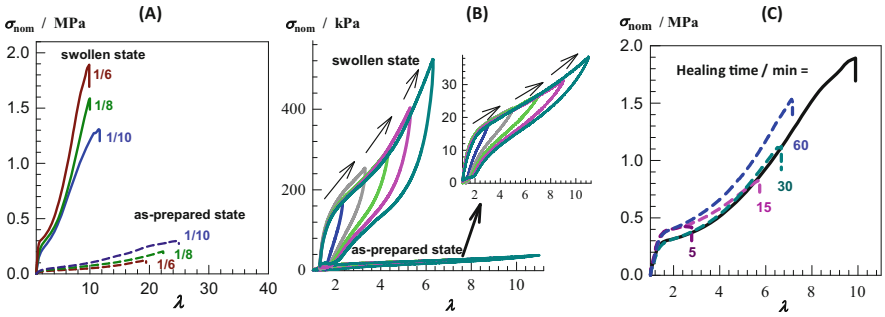

Fig. 15 (**a**) Tensile stress-strain curves of as-prepared (dashed curves) and water-swollen PAAc hydrogels (solid curves) formed at various CTAB/AAc mole ratios (β_o) as indicated. $C_o = 30$ w/v%. (**b**) Five-step tensile cycles with increasing maximum strain conducted on a PAAc hydrogel specimen in its as-prepared and swollen states. The inset is a zoom-in to the data of the as-prepared hydrogel. $C_o = 20$ w/v%. $\beta_o = 1/8$. (**c**) Tensile stress-strain curves of virgin (solid curve) and healed PAAc hydrogels (dashed curves) in their swollen states in water at various healing times as indicated. $C_o = 30$ w/v%. $\beta_o = 1/6$. From [117] with permission from the American Chemical Society

cross-links appear due to the formation of aggregates composed of oppositely charged AAc and CTA ions and alkyl side chains of C17.3 segments. These second cross-links lead to a dramatic increase in the mechanical properties of water-swollen PAAc hydrogels during which their viscous, energy-dissipating properties do not change [117]. Figure 15a shows tensile stress-strain curves of as-prepared (dashed curves) and water-swollen PAAc hydrogels (solid curves) formed at a constant AAc concentration (C_o) of 30 w/v % but at various CTAB/AAc mole ratios (β_o) as indicated. Young's modulus and tensile strength increase up to 23- and 14-fold, respectively, while stretch at break decreases by two- to threefold after swelling of the hydrogels in water. PAAc hydrogels formed at $C_o = 30$ w/v% and $\beta_o = 1/6$ in their equilibrium swollen state with 55% water exhibit the highest Young's modulus (0.61 MPa), tensile strength (1.7 MPa), and a pretty good stretchability (900%).

Figure 15b shows the results of five-step tensile cyclic tests with increasing maximum strain conducted on a PAAc hydrogel specimen in its as-prepared and swollen states. In contrast to the SDS-containing nonionic hydrogels [38], PAAc hydrogels formed in the presence of the oppositely charged surfactant CTAB exhibit reversible mechanical cycles in both their as-prepared and swollen states revealing that their physical cross-links break reversibly under loading. Cut-and-heal tests indeed show self-healing ability of PAAc hydrogels. All hydrogels in their as-prepared states exhibit autonomic self-healing at 24°C within a few minutes. Hydrogels in their swollen states could also be healed after treatment of the cut region with an aqueous solution of worm-like CTAB micelles at 35°C which provides dissociation of PAAc-CTAB complexes, followed by washing the cut region with water to remove free surfactants. After a healing time of 60 min, the hydrogels formed at $C_o = 30$ w/v%, and $\beta_o = 1/6$ sustains 1.5 MPa stresses at 600% elongation (Fig. 15c).

3.2.2 Hydrogels Containing Crystalline Domains

Another attempt to fabricate mechanically strong hydrophobically modified hydrogels with self-healing ability was to create alkyl crystal cross-links in the gel network providing temperature-induced hard-to-soft transitions and thereby self-healing [27, 128]. Thus, when the local temperature of the damaged area of a semicrystalline physical hydrogel is increased above the crystalline melting temperature, the crystalline order is lost along with the strength of the crystal cross-links providing a rapid healing due to the increased chain mobility in that area. Preparation of semicrystalline chemically cross-linked hydrogels and the observation of an order-to-disorder transition in the gel network were first reported 25 years ago by Osada et al. [129–132]. They fabricated hybrid hydrogels containing both chemical and alkyl crystal cross-links by free-radical copolymerization of AAc and C18A in the presence of the chemical cross-linker BAAm in ethanol, a common solvent for both monomers. The amorphous hydrophilic region of the hydrogels provides water absorption, while the crystalline region is responsible for their high modulus. The alkyl crystals have a short range ordering with a d_1 spacing of around 0.42 nm corresponding to side-by-side packing of n-octadecyl (C18) side chains (Fig. 16A). In addition, a long-range ordering was also observed with a d_2 spacing of 6.3 nm, which is around twice the fully stretched length of C18, revealing non-interdigitated, tail-to-tail alignment of alkyl side chains (Fig. 16a). This type of alignment in semicrystalline hydrogels is in contrast to comb-like polymers with alkyl side chains

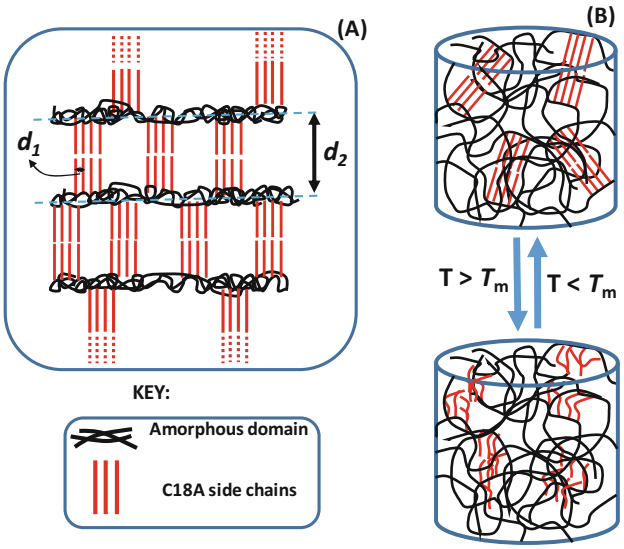

Fig. 16 (**a**) Scheme showing alkyl crystals and amorphous regions in semicrystalline hydrogels based on hydrophilic monomers and N-alkyl (meth)acrylates. From [127] with permission from the American Chemical Society. (**b**) Scheme showing melting of alkyl crystals to form hydrophobic associations and their recrystallization below T_m

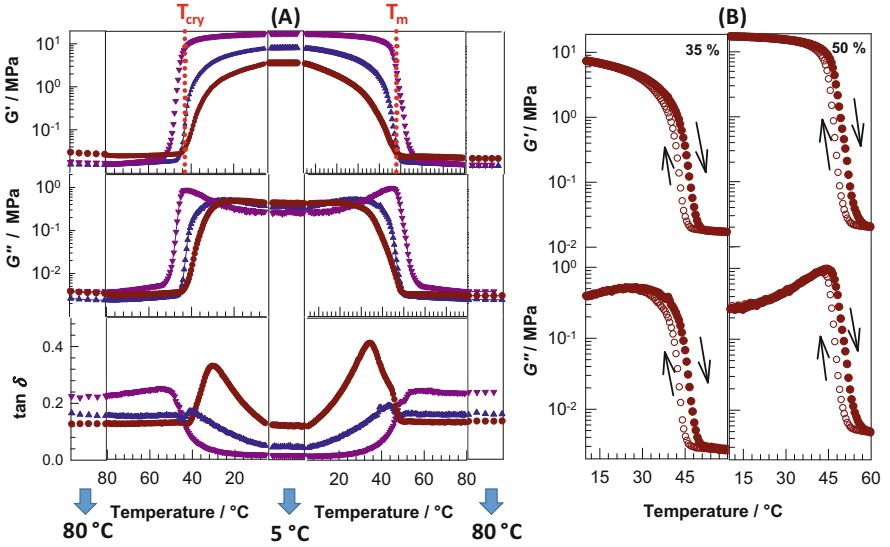

Fig. 17 (**a**) Temperature-dependent variations of the dynamic moduli G' and G'' and tan δ of semicrystalline hybrid PAAc hydrogels with varying amount of C18A during a thermal cycle between 80 and 5°C. C18A = 20 (●), 35 (▲), and 50 mol% (▼). BAAm = 1 mol%. (**b**) G' and G'' of PAAc hydrogels with 35 (left panel) and 50 mol% C18A (right panel) during the thermal cycle. Down and up arrows indicate increasing and decreasing temperatures, respectively. $\omega = 6.28$ rad s^{-1}. $\gamma_o = 0.1\%$. From [91] with permission from the American Chemical Society

forming an interdigitated side chain structure [110, 133, 134]. Hybrid semicrystalline hydrogels undergo up to 120-fold reversible change in their modulus by changing the temperature between below and above the crystalline melting temperature [129].

Later on, semicrystalline hybrid hydrogels of Osada et al. were synthesized via micellar polymerization in aqueous solutions of WLMs instead of the solution polymerization in ethanol [91]. The block-like structure of poly(AAc-co-C18A) copolymer chains formed in a micellar solution enhances the hydrophobic interactions leading to two to three orders of magnitude change in the storage modulus in response to a change in the temperature. Figure 17a shows temperature-dependent variations of G', G'', and tan δ during a thermal cycle between 80 and 5°C for PAAc hydrogels formed via micellar polymerization with 1 mol% BAAm and varying amounts of C18A between 20 and 50 mol%. The dotted vertical lines in the upper panel indicate the melting T_m and recrystallization temperatures T_{cry}. The hydrogels at 5°C exhibit a storage modulus G' in the MPa level, i.e., 3.6, 8, and 17.6 MPa for 20, 35, and 50 mol% C18A, respectively. During heating, G' drastically decreases at around T_m, 48 ± 2°C, and attains a value between 16 and 27 kPa at 80°C, which is 130- to 700-fold smaller than the initial modulus at 5°C [91]. The temperature-induced modulus change is totally reversible as such upon cooling, G' rapidly increases at around T_{cry}, 43 ± 2°C, to attain the initial MPa level modulus (Fig. 17b) [91].

To generate self-healing in semicrystalline hydrogels, they were recently prepared in the absence of a chemical cross-linker by micellar, bulk, and solution polymerizations using several hydrophobic and hydrophilic comonomer pairs [27, 128, 135, 136]. Because of the cooperative H-bonding and hydrophobic interactions, AAc/C18A comonomer pair leads to the formation of hydrogels with the highest melting temperature (48–56°C), degree of crystallinity (10–33%), Young's modulus (up to 308 ± 16 MPa), and tensile strength (up to 5.1 ± 0.1 MPa) [135]. Compressive mechanical tests conducted on virgin and cut-repaired hydrogels reveal extraordinary self-healing capability of the hydrogels. The healing of the hydrogels was induced by heating locally the cut region above T_m followed by pressing the cut surfaces together and finally cooling below T_m to reform alkyl crystals bridging the cut surfaces (Fig. 16b). Healed DMAA/C18A hydrogels with 50 mol% C18A exhibit a compressive strength of 138 ± 10 MPa, which is around 87% of the virgin ones [135]. Moreover, the healing can also be induced by internal heating using laser light if the hydrogel contains gold nanoparticles that generate heat due to the surface plasmon resonance [137]. On/off switching of the laser light provides melting and recrystallization of alkyl crystals in the damaged area resulting in healing of the hydrogel. Instead of the temperature-induced healing, treatment of the cut surfaces with ethanol was also reported which provides solubilization of the cut surfaces to allow merging the surfaces together [136].

One disadvantage of highly crystalline hydrogels prepared from hydrophilic and hydrophobic monomers is their low stretchability due to the existence of stiff and strong alkyl crystals. One may apparently overcome this drawback by changing the tensile testing parameters, i.e., by reducing the strain rate to provide enough time for the relaxation processes in the physical network. For instance, the toughness and stretch at break of DMAA/C18A hydrogels increase by five- and sevenfold, respectively, when the strain rate is reduced from 7.8×10^{-3} to 4×10^{-3} s^{-1} (Fig. 18a) [135]. However, a versatile alternative strategy to induce such a brittle-to-tough transition without changing the testing parameters is to incorporate hydrophobic monomers with relatively short alkyl side chains creating mobility in the gel network [128]. Figure 18b shows the effect of the non-crystallizable, weak hydrophobe C12M on the stress-strain curves of DMAA/C18A hydrogels at a fixed strain rate. The hydrogels were prepared at a fixed content of the hydrophobes (30 mol%) but at various fractions of C12M between 0.1 and 20 mol%. In the absence of C12M, the hydrogel ruptures in a brittle fashion, as seen by the blue thick curve labeled by "0" in the inset to the figure. However, incorporation of a small amount of C12M induces significant yielding accompanied with a brittle-to-ductile transition. For instance, without and with 0.2 mol% C12M, the hydrogels exhibit almost identical Young's moduli E, i.e., 71 ± 3 and 70 ± 5 MPa, respectively, indicating that the cross-link density is not effected from the added amount of C12M. However, this tiny amount of C12M affects considerably the ultimate mechanical properties of the hydrogels. The hydrogel without C12M ruptures at 20% stretch, while that with 0.2 mol% C12M sustains eightfold larger stretches (167%) and exhibits tenfold larger toughness (9.6 ± 0.3 vs 1.0 ± 0.2 MJ m^{-3}) [128]. Moreover, the highest yield stress σ_y of 7.3 MPa was observed after incorporation of the smallest amount of C12M

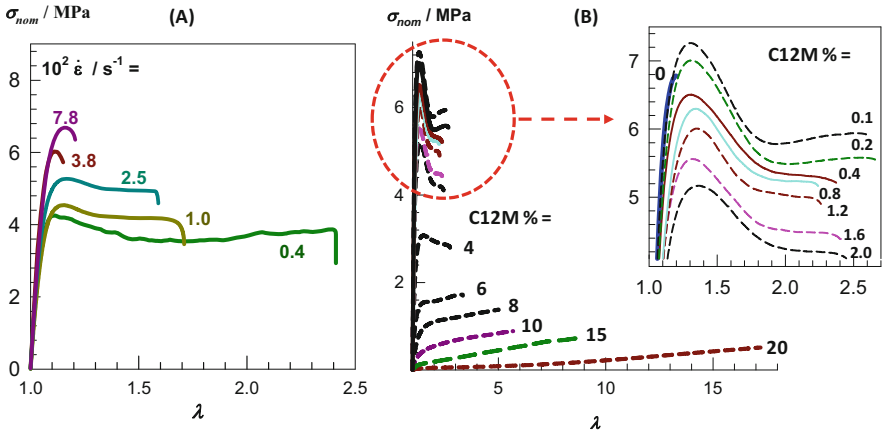

Fig. 18 Stress-strain curves of DMAA/C18A hydrogels at various strain rates $\dot{\varepsilon}$ (**a**) and at various C12M contents (**b**). (**a**) C18A = 30 mol%. From [135] with permission from Elsevier. (**b**) $\dot{\varepsilon} = 8.3 \times 10^{-2}\ s^{-1}$. C18A + C12M = 30 mol%. C12M contents are indicated. The inset is a zoom-in to the curves of the hydrogels with C12M contents below 4 mol%. From [128] with permission from the American Chemical Society

(0.1 mol%) into the polymer backbone, which is close to the tensile strength of C12M-free hydrogel. σ_y linearly decreases with increasing C12M content by the equation, $\sigma_y = 7.1 \pm 0.1 - \text{C12M mol\%}$, indicating that the weak hydrophobe C12M increases the number of mobile segments in the hydrogels and hence enhances the molecular mobility between crystalline regions. We have to mention the modulus and the fracture stress rapidly decrease above 2 mol% C12M due to a significant decrease in the degree of crystallinity leading to highly stretchable but mechanically weak hydrogels (Fig. 18b).

The significant effect of a weak hydrophobe on the ultimate mechanical properties of semicrystalline hydrogels was explained with the formation of more ordered and thinner alkyl crystals, as demonstrated by SAXS measurements [128]. During stretching of the hydrogels containing strong and weak hydrophobic segments, lamellar clusters formed from layered alkyl crystals appear that are interconnected by tie molecules. The tie molecules in amorphous domains create an energy dissipation mechanism by transmission of the external load between the lamellar clusters leading to their bending and finally breaking at the yield point [138–140]. Because lamellar clusters are physical in nature, they could be repaired by heating above T_m followed by cooling. The solid and dotted curves in Fig. 19a present two successive loading curves up to a 100% stretch ratio for a DMAA/C18A hydrogel specimen prepared in the presence of 0.4 mol% C12M [128]. According to the first loading curve, Young's modulus E and yield stress σ_f are 68 and 6.5 MPa, respectively (Fig. 19b). The modulus significantly decreases, and yielding disappears during the second loading indicating the occurrence of an irreversible damage in the lamellar clusters. However, repairing the clusters by the heating-cooling treatment as

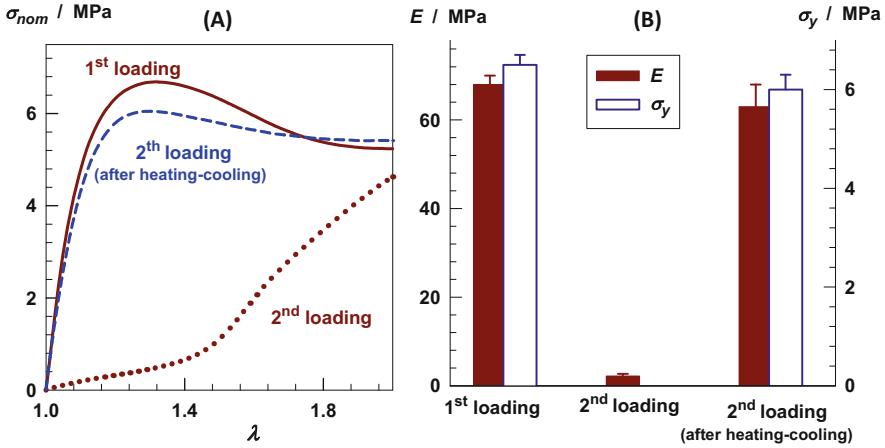

Fig. 19 (**a**) Two successive stress-strain curves up to an elongation ratio $\lambda = 2$ for a DMAA/C18A hydrogel specimen containing 0.4 mol% C12M. The second loading was conducted immediately after the first one (dotted curve) and after the heating-cooling treatment (dashed curve). $\dot{\varepsilon} = 8.3 \times 10^{-2}\ s^{-1}$. (**b**) Young's modulus E and yield stress σ_y of the hydrogel calculated from the first and second loading steps. From [128] with permission from the American Chemical Society

mentioned above and then conducting the second loading almost completely recovers the mechanical properties of the virgin hydrogel (Figs. 19a, b). The self-healing efficiency is 93% with respect to the modulus (63 ± 5 MPa) and yield stress (6.0 ± 0.4) [128].

Semicrystalline physical hydrogels were also fabricated with a macroscopically anisotropic structure consisting of hard and soft regions joined together through a strong interface [141]. Such segmented hydrogel structures mimic many biological systems such as the intervertebral disk (IVD) which provides flexibility, load transfer, and energy dissipation to the spine. IVD consists of a soft inner core, called nucleus pulposus, surrounded by mechanically strong annulus fibrosus [142, 143]. This structural design provides IVD an extraordinary mechanical performance, as such it can withstand millions of loading cycles over the human lifespan. Another example is the enthesis, the connective tissue between the tendon/ligament and bone, which not only acts as a connector of soft-to-hard tissue but also reduces the risk of damage under stress [144]. The synthetic strategy of semicrystalline segmented hydrogels bases on the stratification of aqueous solutions even at very low density differences, as observed in many seas and lakes [141]. For example, Fig. 20a shows two monomer mixtures composed of DMAA together with 30 mol% C18A (red) and 50 mol% C12M (blue). The slightly lower density of the blue mixture by 0.6% provides formation of two liquid layers if blue mixture is dropwise added on top of the red one, as seen in the upper panel of Fig. 20a. Otherwise, if red mixture is dropped on top of the blue one, they mix completely in a short period of time (bottom panel). In this way, layered monomer mixtures

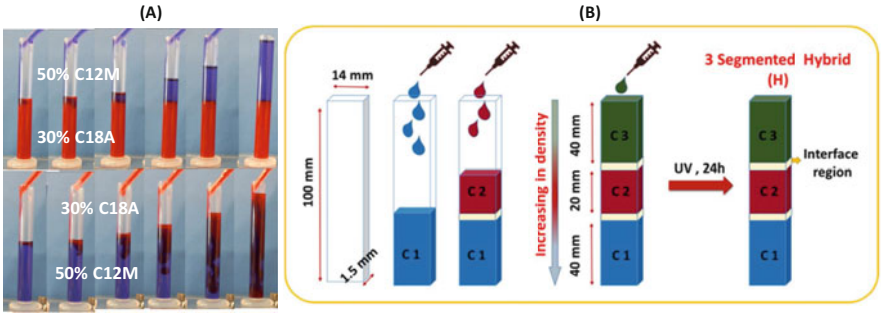

Fig. 20 (**a**) Stratification of the monomer mixtures composed of DMAA together with 30 mol% C18A (red) and 50 mol% C12M (blue). Two liquid layers only form when red solution is on the bottom due to its slightly higher density. (**b**) Synthetic procedure for the fabrication of segmented hydrogels. From [145] with permission from Wiley

containing photoinitiators were prepared and then subjected to UV polymerization to obtain two or more segmented semicrystalline hydrogels (Fig. 20b) [141, 145].

Figure 21a presents the photograph of a dumbbell-shaped segmented hydrogel specimen consisting of C1 and C3 components. C1 and C3 have a common PDMAA backbone, but they contain 30 mol% C18A and 50 mol% C12M hydrophobic units, respectively. Thus, C1 is a semicrystalline hydrogel with $T_m = 48°C$ and exhibits a high modulus E (54 MPa), a tensile strength σ_f (5 MPa), and a low stretchability ε_f (79%), whereas C3 is an amorphous hydrogel due to the relatively short alkyl side chain of C12M. C3 has a low modulus and tensile strength of around 0.1 MPa but a high stretchability (1,140%). DSC scans conducted at the interface region reveal that the melting peak of C1 at 48°C gradually disappears by moving from C1 to C3 part through the interface indicating perfect fusion of the two hydrogel segments (Fig. 21b) [141]. Figure 20c, d shows stress-strain curves and mechanical parameters of C1 and C3 segments and the interface region of C1/C3 hybrid. The interface region exhibits the average properties of both segments and hence has a higher modulus and tensile strength as compared to the C3 segment. As a consequence, when C1/C3 hydrogel is subjected to tensile testing, the interface remains intact, while it ruptures at C3 segment (Fig. 21e) [141]. Thus, despite large mismatches in the mechanical properties of C1 and C3 segments, stratification technique provides a smooth interface that remains stable under loading. Two- and three-segmented hydrogels with various chemical compositions and mechanical properties have been reported recently [141, 145]. Because of the physical nature of segmented hydrogels, they all exhibit self-healing behavior after heating-cooling treatment of the damaged areas.

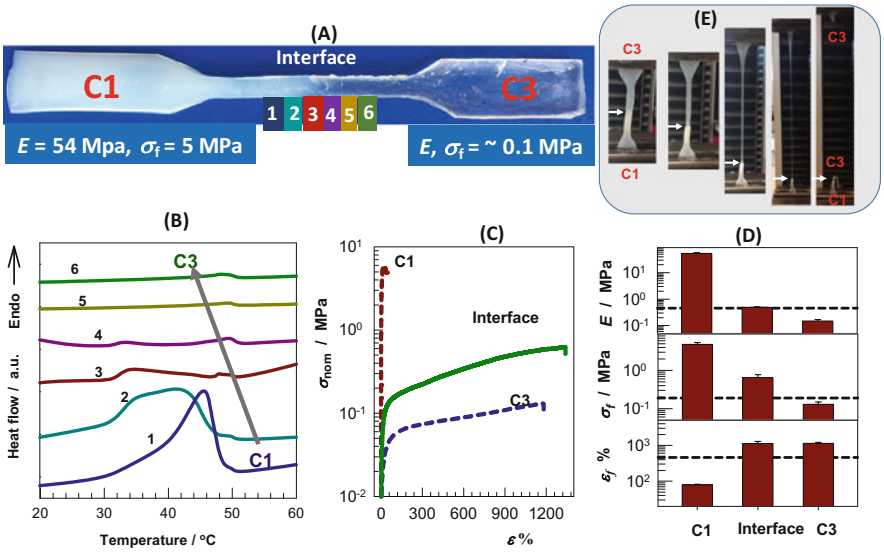

Fig. 21 (**a**) Photograph a dumbbell-shaped hybrid hydrogel composed of C1 and C3 segments whose mechanical parameters are indicated. (**b**) DSC scans performed at the interface region of segmented C1/C3 hydrogel. The numbers correspond to the location numbers in (**a**). (**c**, **d**) Tensile stress-strain curves of C1 and C3 components and the interface of segmented C1/C3 hydrogel together with their Young's modulus E, tensile strength σ_f, and stretch at break ε_f. The horizontal dashed lines in the right panel show the respective values for the segmented hydrogel. (**e**) Photograph during the mechanical tests of C1/C3 hydrogel. The interface regions are indicated by the white arrows. From [141] with permission from the American Chemical Society

4 Conclusions and Outlook

Recent developments in the field of hydrogels enable to enhance their mechanical strength to MPa level at a water content between 60 and 75 wt%, which is similar to the load-bearing tissues. Another challenge immersing in the last years is to generate self-healing function in such hydrogels without affecting their good mechanical properties. Because self-healing and mechanical strength are inversely related, autonomic self-healing in high-strength hydrogels formed by long-lived cross-links could not been created. However, a significant hard-to-soft or first-order transition induced by an external trigger creates self-healing in such high-strength hydrogels and hence combines the two antagonistic features in a single hydrogel material. In this review, I mainly focused on hydrogels formed via H-bonding and hydrophobic interactions, which are generally highly stretchable and exhibit Young's modulus and tensile strength in the range of MPa.

The strategies developed so far for the fabrication of H-bonded hydrogels are based on forming self-complementary dual or multiple H-bonding interactions between polymer chains. In addition, hydrophobic segments have been incorporated into the hydrophilic chains to amplify these interactions. Polymer chains consisting

of H-bond acceptor and donor segments, dual amide groups, UPy moieties, and DAT-DAT interactions create high-strength H-bonded hydrogels with self-healing or self-recovery functions. Such hydrogels with 40–80 wt% water exhibit a Young's modulus up to 84 MPa and sustain 1–5 MPa tensile stresses at 800–1,400% elongations. H-bonded hydrogels prepared by polymerization of NAGA monomer with dual amide groups in aqueous solutions exhibit the highest stretchability, while those formed by combination of hydrophobic and H-bonding interactions via UPy and C18A units, respectively, have the highest tensile strength. DMAA and MAAc are attractive H-bond acceptor and donor monomers, respectively, for the preparation of H-bonded hydrogels. As compared to AAm, DMAA has an enhanced H-bond acceptor capability through their carbonyl groups via σ-donation effect of the methyl groups contributing to the H-bonding cooperativity in hydrogels when it is copolymerized with H-donor monomers. Moreover, the use of MAAc instead of AAc as a H-bond donor monomer significantly improves the mechanical performance of H-bonded hydrogels due to the hydrophobic interactions of the α-methyl groups of MAAc units. The primary chain length of H-bonded hydrogels is also effective in determining their mechanical strength due to the proximity effect. Increasing the chain length of the primary chains facilitates formation of H-bonds in the vicinity of preexisting H-bonds contributing H-bond cooperativity leading to high-strength hydrogels. Recently developed H-bonded hydrogels capable of absorbing a large amount of water (~1,700 g g^{-1}) and those containing ds-DNA in a clay environment are attractive self-healing soft materials for various applications such as superabsorbent polymers and in gene delivery systems, respectively.

Hydrophobic interactions between hydrophobically modified polymers in an aqueous environment lead to the formation of hydrogels containing crystalline domains and/or hydrophobic associations acting as strong and weak physical cross-links, respectively. Such hydrogels have recently been prepared using bulk, solution, and micellar copolymerization of a variety of hydrophilic and hydrophobic monomers via free-radical mechanism. The feed molar ratio of the monomers, alkyl side chain length of the hydrophobes, type of the hydrophilic monomer, water content, and the presence of surfactant micelles are the main experimental parameters providing precise control of the mechanical, viscoelastic, and self-healing properties of the hydrogels. When the hydrophobe content is limited to 2 mol%, SDS-containing self-healing hydrogels obtained from DMAA and C17.3M exhibit the highest stretchability (4,200 ± 400%) due to the associative behavior of DMAA segments. They also exhibit a complete self-healing without any external stimuli at 24°C within 20 min. Replacing nonionic DMAA with the anionic AAc monomer and SDS with the cationic CTAB surfactant produces physical hydrogels of high tensile strength (1.7 MPa) due to the dual hydrophobic and ionic interactions. Moreover, a significant mechanical property improvement in the hydrogels could be achieved when the hydrophobe content is increased above 10 mol% providing formation of crystalline domains in addition to the hydrophobic associations. AAc/C18A comonomer produces semicrystalline hydrogels with the highest melting temperature (48–56°C), degree of crystallinity (10–33%), Young's modulus (up to 308 ± 16 MPa), and tensile strength (up to 5.1 ± 0.1 MPa). Damaged hydrogels with

50 mol% C18A after heating-induced healing exhibit a compressive strength of 138 ± 10 MPa, which is around 87% of the virgin ones. Semicrystalline hydrogels can also be made highly stretchability when a small amount of non-crystallizable units are incorporated in the gel network to create mobility.

Research directed toward synthesis of self-healing hydrogels provided several important findings not only in the field of self-healing but also in other hydrogel applications. For instance, the presence of surfactants in hydrophobically modified hydrogels significantly changes their viscoelastic and mechanical properties. Surfactant micelles solubilize hydrophobic associations and alkyl crystals and hence facilitate the diffusion of polymer chains, thereby inducing self-healing. They are also able to solubilize semicrystalline hydrogels of high mechanical strength opening up their applications as injectable gels and as smart inks for 3D or 4D printing. Similarly, H-bonded self-healing hydrogels dissolve in aqueous urea solutions, while the injectable solution thus formed turns into a gel when the urea is forced to diffuse out of the solution. The viscoelastic and mechanical properties of H-bonded and hydrophobically modified hydrogels can be tailored by aqueous urea solutions or surfactant micelles, respectively, to fit a variety of needs. Thus, urea- or surfactant-induced processability may provide several future applications of high-strength H-bonded and hydrophobically modified physical hydrogels.

Acknowledgment Work was partially supported by the Turkish Academy of Sciences (TUBA). The author would like to thank all collaborators and graduate students for their contributions in the development of hydrophobically modified and H-bonded physical hydrogels.

References

1. Calvert P (2009) Hydrogels for soft machines. Adv Mater 21:743–756
2. Means AK, Grunlan MA (2019) Modern strategies to achieve tissue-mimetic, mechanically robust hydrogels. ACS Macro Lett 8:705–713
3. Chai Q, Jiao Y, Yu X (2017) Hydrogels for biomedical applications: their characteristics and the mechanisms behind them. Gels 3(1). pii: E6
4. Hoare TR, Kohane DS (2008) Hydrogels in drug delivery: progress and challenges. Polymer 49:1993–2007
5. Brown HR (2007) A model of the fracture of double network gels. Macromolecules 40:3815–3818
6. Gong JP (2010) Why are double network hydrogels so tough? Soft Matter 6:2583–2590
7. Zhao X (2014) Multi-scale multi-mechanism design of tough hydrogels: building dissipation into stretchy networks. Soft Matter 10:672–687
8. Creton C, Ciccotti M (2016) Fracture and adhesion of soft materials: a review. Rep Prog Phys 79:056601
9. Creton C (2017) 50th anniversary perspective: networks and gels: soft but dynamic and tough. Macromolecules 50:8297–8316
10. Fu J (2018) Strong and tough hydrogels crosslinked by multi-functional polymer colloids. J Polym Sci Part B Polym Phys 56:1336–1350
11. Fu J, in het Panhuis M (2019) Hydrogel properties and applications. J Mater Chem B 7:1523–1525

12. Wu F, Chen L, Li Y, Lee KI, Fei B (2017) Super-tough hydrogels from shape-memory polyurethane with wide-adjustable mechanical properties. J Mater Sci 52:4421–4434
13. Gong JP, Katsuyama Y, Kurokawa T, Osada Y (2003) Double-network hydrogels with extremely high mechanical strength. Adv Mater 15:1155–1158
14. Tuncaboylu DC, Sarı M, Oppermann W, Okay O (2011) Tough and self-healing hydrogels formed via hydrophobic interactions. Macromolecules 44:4997–5005
15. Uzumcu AT, Guney O, Okay O (2018) Highly stretchable DNA/clay hydrogels with self-healing ability. ACS Appl Mater Interfaces 10:8296–8306
16. Hager MD, van der Zwaag S, Schubert US (eds) (2016) Self-healing materials. Adv Polym Sci 273. 413 pp
17. Taylor DL, in het Panhuis M (2016) Self-healing hydrogels. Adv Mater 28:9060–9093
18. Gyarmati B, Szilágyi BA, Szilágyi A (2017) Reversible interactions in self-healing and shape memory hydrogels. Eur Polym J 93:642–669
19. Okay O (2015) Self-healing hydrogels formed via hydrophobic interactions. Adv Polym Sci 268:101–142
20. Okay O (2019) Semicrystalline physical hydrogels with shape-memory and self-healing properties. J Mater Chem B 7:1581–1596
21. Talebian S, Mehrali M, Taebnia N, Pennisi CP, Kadumudi FB, Foroughi J, Hasany M, Nikkhah M, Akbari M, Orive G, Dolatshahi-Pirouz A (2019) Self-healing hydrogels: the next paradigm shift in tissue engineering? Adv Sci 6:1801664. (1–47)
22. Li Q, Liu C, Wen J, Wu Y, Shan Y, Liao J (2017) The design, mechanism and biomedical application of self-healing hydrogels. Chin Chem Lett 28:1857–1874
23. Strandman S, Zhu XX (2016) Self-healing supramolecular hydrogels based on reversible physical interactions. Gels 2:16. (1–31)
24. Wang W, Zhang Y, Liu W (2017) Bioinspired fabrication of high strength hydrogels from non-covalent interactions. Prog Polym Sci 71:1–25
25. Sun TL, Kurokawa T, Kuroda S, Ihsan AB, Akasaki T, Sato K, Haque MA, Nakajima T, Gong JP (2013) Physical hydrogels composed of polyampholytes demonstrate high toughness and viscoelasticity. Nat Mater 12:932–937
26. Sun TL, Cui K (2020) Tough and self-healing hydrogels from polyampholytes. Adv Polym Sci (in press), https://doi.org/10.1007/12_2019_56
27. Bilici C, Can V, Nöchel U, Behl M, Lendlein A, Okay O (2016) Melt-processable shape-memory hydrogels with self-healing ability of high mechanical strength. Macromolecules 49:7442–7449
28. Su E, Okay O (2019) A self-healing and highly stretchable polyelectrolyte hydrogel via cooperative hydrogen-bonding as a superabsorbent polymer. Macromolecules 52:3257–3267
29. Dai X, Zhang Y, Gao L, Bai T, Wang W, Cui Y, Liu W (2015) A mechanically strong, highly stable, thermoplastic, and self-healable supramolecular polymer hydrogel. Adv Mater 27:3566–3571
30. Wang H, Zhu H, Fu W, Zhang Y, Xu B, Gao F, Cao Z, Liu W (2017) A high strength self-healable antibacterial and anti-inflammatory supramolecular polymer hydrogel. Macromol Rapid Commun 38:1600695
31. Tang L, Liu W, Liu G (2010) High-strength hydrogels with integrated functions of H-bonding and thermoresponsive surface-mediated reverse transfection and cell detachment. Adv Mater 22:2652–2656
32. Gao H, Wang N, Hu X, Nan W, Han Y, Liu W (2013) Double hydrogen-bonding pH-sensitive hydrogels retaining high-strengths over a wide pH range. Macromol Rapid Commun 34:63–68
33. Maly KE, Dauphin C, Wuest JD (2006) Self-assembly of columnar mesophases from diaminotriazines. J Mater Chem 16:4695–4700
34. Liu B, Liu W (2018) Poly(vinyl diaminotriazine): from molecular recognition to high-strength hydrogels. Macromol Rapid Commun 39:1800190
35. Sijbesma RP, Meijer EW (2003) Quadruple hydrogen bonded systems. Chem Commun:5–16

36. Guo M, Pitet LM, Wyss HM, Vos M, Dankers PYW, Meijer EW (2014) Tough stimuli-responsive supramolecular hydrogels with hydrogen-bonding network junctions. J Am Chem Soc 136:6969–6977
37. Jeon I, Cui J, Illeperuma WRK, Aizenberg J, Vlassak JJ (2016) Extremely stretchable and fast self-healing hydrogels. Adv Mater 28:4678–4683
38. Tuncaboylu DC, Sahin M, Argun A, Oppermann W, Okay O (2012) Dynamics and large strain behavior of self-healing hydrogels with and without surfactants. Macromolecules 45:1991–2000
39. Mihajlovic M, Wyss HM, Sijbesma RP (2018) Effects of surfactant and urea on dynamics and viscoelastic properties of hydrophobically assembled supramolecular hydrogel. Macromolecules 51:4813–4820
40. Chang X, Geng Y, Cao H, Zhou J, Tian Y, Shan G, Bao Y, Wu ZL, Pan P (2018) Dual-crosslink physical hydrogels with high toughness based on synergistic hydrogen bonding and hydrophobic interactions. Macromol Rapid Commun 39:e1700806
41. Hu X, Vatankhah-Varnoosfaderani M, Zhou J, Li Q, Sheiko SS (2015) Weak hydrogen bonding enables hard, strong, tough, and elastic hydrogels. Adv Mater 27:6899–6905
42. Ding H, Zhang XN, Zheng SY, Song Y, Wu ZL, Zheng Q (2017) Hydrogen bond reinforced poly(1-vinylimidazole-co-acrylic acid) hydrogels with high toughness, fast self-recovery, and dual pH responsiveness. Polymer 131:95–103
43. Zhang XN, Wang YJ, Sun S, Hou L, Wu P, Wu ZL, Zheng Q (2018) A tough and stiff hydrogel with tunable water content and mechanical properties based on the synergistic effect of hydrogen bonding and hydrophobic interaction. Macromolecules 51:8136–8146
44. Song G, Zhang L, He C, Fang D-C, Whitten PG, Wang H (2013) Facile fabrication of tough hydrogels physically cross-linked by strong cooperative hydrogen bonding. Macromolecules 46:7423–7435
45. Kriz J, Dybal J, Brus J (2006) Cooperative hydrogen bonds of macromolecules. 2. Two-dimensional cooperativity in the binding of poly(4-vinylpyridine) to poly (4-vinylphenol). J Phys Chem B 110:18338–18346
46. Kriz J, Dybal J (2007) Cooperative hydrogen bonds of macromolecules. 3. A model study of the proximity effect. J Phys Chem B 111:6118–6126
47. Durmaz S, Okay O (2000) Acrylamide/2-acrylamido-2-methyl propane sulfonic acid sodium salt -based hydrogels: synthesis and characterization. Polymer 41:3693–3704
48. Xing A, Li L, Wang T, Ding Y, Liu G, Zhang G (2014) A self-healing polymeric material: from gel to plastic. J Mater Chem A 2:11049–11053
49. Su E, Okay O (2018) Hybrid cross-linked poly(2-acrylamido-2-methyl-1-propanesulfonic acid) hydrogels with tunable viscoelastic, mechanical and self-healing properties. React Funct Polym 123:70–79
50. Weng L, Gouldstone A, Wu Y, Chen W (2008) Mechanically strong double network photocrosslinked hydrogels from N,N-dimethylacrylamide and glycidyl methacrylated hyaluronan. Biomaterials 29:2153–2163
51. Wang F, Yong X, Deng J, Wu Y (2018) Poly(N,N-dimethylacrylamide-octadecyl acrylate)-clay hydrogels with high mechanical properties and shape memory ability. RSC Adv 8:16773–16780
52. Li W, Li J, Gao J, Li B, Xia Y, Meng Y, Yu Y, Chen H, Dai J, Wang H, Guo Y (2011) The fine-tuning of thermosensitive and degradable polymer micelles for enhancing intracellular uptake and drug release in tumors. Biomaterials 32:3832–3844
53. Babic M, Horak D, Jendelova P, Glogarova K, Herynek V, Trchova M, Likavcanova K, Lesny P, Pollert E, Hajek M, Sykova E (2009) Poly(N,N-dimethylacrylamide)-coated maghemite nanoparticles for stem cell labeling. Bioconjug Chem 20:283–294
54. De Queiroz AAA, Castro SC, Higa OZ (1997) Adsorption of plasma proteins to DMAA hydrogels obtained by ionizing radiation and its relationship with blood compatibility. J Biomater Sci Polym Edn 8:335–347

55. Yang D, Peng S, Hartman MR, Gupton-Campolongo T, Rice EJ, Chang AK, Gu Z, Lu GQ, Luo D (2013) Enhanced transcription and translation in clay hydrogel and implications for early life evolution. Sci Rep 3:3165
56. Cai P, Huang Q-Y, Zhang X-W (2006) Interactions of DNA with clay minerals and soil colloidal particles and protection against degradation by DNase. Environ Sci Technol 40:2971–2976
57. Haraguchi K, Takehisa T (2002) Nanocomposite hydrogels: a unique organic–inorganic network structure with extraordinary mechanical, optical, and swelling/de-swelling properties. Adv Mater 14:1120–1124
58. Haraguchi K, Takehisa T, Fan S (2002) Effects of clay content on the properties of nanocomposite hydrogels composed of poly(N-isopropylacrylamide) and clay. Macromolecules 35:10162–10171
59. Haraguchi K, Farnworth R, Ohbayashi A, Takehisa T (2003) Compositional effects on mechanical properties of nanocomposite hydrogels composed of poly(N, N-dimethylacrylamide) and clay. Macromolecules 36:5732–5741
60. Haraguchi K, Li H-J, Matsuda K, Takehisa T, Elliott E (2005) Mechanism of forming organic/inorganic network structures during in-situ free-radical polymerization in PNIPA−clay nanocomposite hydrogels. Macromolecules 38:3482–3490
61. Klein A, Whitten PG, Resch K, Pinter G (2015) Nanocomposite hydrogels: fracture toughness and energy dissipation mechanisms. J Polym Sci Part B Polym Phys 53:1763–1773
62. Okay O, Oppermann W (2007) Polyacrylamide – clay nanocomposite hydrogels: rheological and light scattering characterization. Macromolecules 40:3378–3387
63. Haraguchi K, Uyama K, Tanimoto H (2011) Self-healing in nanocomposite hydrogels. Macromol Rapid Commun 32:1253–1258
64. Mongondry P, Tassin J-F, Nicolai T (2005) Revised state diagram of Laponite dispersions. J Colloid Interface Sci 283:397–405
65. Mongondry P, Nicolai T, Tassin J-F (2004) Influence of pyrophosphate or polyethylene oxide on the aggregation and gelation of aqueous Laponite dispersions. J Colloid Interface Sci 275:191–196
66. Topuz F, Okay O (2009) Formation of hydrogels by simultaneous denaturation and cross-linking of DNA. Biomacromolecules 10:2652–2661
67. Karacan P, Okay O (2013) Ethidium bromide binding to DNA cryogels. React Funct Polym 73:442–450
68. Pan W, Wen H, Niu L, Su C, Liu C, Zhao J, Mao C, Liang D (2016) Effects of chain flexibility on the properties of DNA hydrogels. Soft Matter 12:5537–5541
69. Topuz F, Okay O (2008) Rheological behavior of responsive DNA hydrogels. Macromolecules 41:8847–8854
70. Zhang Y, Li Y, Liu W (2015) Dipole-dipole and H-bonding interactions significantly enhance the multifaceted mechanical properties of thermoresponsive shape memory hydrogels. Adv Funct Mater 25:471–480
71. Wang YJ, Li CY, Wang ZJ, Zhao Y, Chen L, Wu ZL, Zheng Q (2018) Hydrogen bond-reinforced double-network hydrogels with ultrahigh elastic modulus and shape memory property. J Polym Sci B 56:1281–1286
72. Yuan T, Cui X, Liu X, Qu X, Sun J (2019) Highly tough, stretchable, self-healing, and recyclable hydrogels reinforced by in situ-formed polyelectrolyte complex nanoparticles. Macromolecules 52:3141–3149
73. Yang J, Xu F, Han CR (2017) Metal ion mediated cellulose nanofibrils transient network in covalently cross-linked hydrogels: mechanistic insight into morphology and dynamics. Biomacromolecules 18:1019–1028
74. Wei Z, He J, Liang T, Oh H, Athas J, Tong Z, Wang C, Nie Z (2013) Autonomous self-healing of poly(acrylic acid) hydrogels induced by the migration of ferric ions. Polym Chem 4:4601–4605

75. Lin P, Ma S, Wang X, Zhou F (2015) Molecularly engineered dual-crosslinked hydrogel with ultrahigh mechanical strength, toughness, and good self-recovery. Adv Mater 27:2054–2059
76. Zhong M, Liu X-Y, Shi F-K, Zhang L-Q, Wang X-P, Cheetham AG, Cui H, Xie X-M (2015) Self-healable, tough and highly stretchable ionic nanocomposite physical hydrogels. Soft Matter 11:4235–4241
77. Shao C, Chang H, Wang M, Xu F, Yang J (2017) High-strength, tough, and self-healing nanocomposite physical hydrogels based on the synergistic effects of dynamic hydrogen bond and dual coordination bonds. ACS Appl Mater Interfaces 9:28305–28318
78. Pan C, Liu L, Chen Q, Zhang Q, Guo G (2017) Tough, stretchable, compressive novel polymer/graphene oxide nanocomposite hydrogels with excellent self-healing performance. ACS Appl Mater Interfaces 9:38052–38061
79. Ghoorchian A, Simon JR, Bharti B, Han W, Zhao X, Chilkoti A, López GP (2015) Bioinspired reversibly cross-linked hydrogels comprising polypeptide micelles exhibit enhanced mechanical properties. Adv Funct Mater 25:3122–3130
80. Chandler D (2005) Interfaces and the driving force of hydrophobic assembly. Nature 437:640–647
81. Sun Y, Liu S, Du G, Gao G, Fu J (2015) Multi-responsive and tough hydrogels based on triblock copolymer micelles as multifunctional macro-crosslinkers. Chem Commun 51:8512–8515
82. Fu J (2020) Triblock copolymer micelle-crosslinked hydrogels. Adv Polym Sci (in press), https://doi.org/10.1007/12_2019_55
83. Hao J, Weiss RA (2011) Viscoelastic and mechanical behavior of hydrophobically modified hydrogels. Macromolecules 44:9390–9398
84. Vogt BD, Weiss RA (2020) Hydrophobically associating hydrogels with microphase-separated morphologies. Adv Polym Sci (in press)
85. Miquelard-Garnier G, Demoures S, Creton C, Hourdet D (2006) Synthesis and rheological behavior of new hydrophobically modified hydrogels with tunable properties. Macromolecules 39:8128–8139
86. Hill A, Candau F, Selb J (1993) Properties of hydrophobically associating polyacrylamides: influence of the method of synthesis. Macromolecules 26:4521–4532
87. Volpert E, Selb J, Francoise C (1998) Associating behaviour of polyacrylamides hydrophobically modified with dihexylacrylamide. Polymer 39:1025–1033
88. Regalado EJ, Selb J, Candau F (1999) Viscoelastic behavior of semidilute solutions of multisticker polymer chains. Macromolecules 32:8580–8588
89. Candau F, Selb J (1999) Hydrophobically-modified polyacrylamides prepared by micellar polymerization. Adv Colloid Interface Sci 79:149–172
90. Gao B, Guo H, Wang J, Zhang Y (2008) Preparation of hydrophobic association polyacrylamide in a new micellar copolymerization system and its hydrophobically associative property. Macromolecules 41:2890–2897
91. Bilici C, Okay O (2013) Shape memory hydrogels via micellar copolymerization of acrylic acid and n-octadecyl acrylate in aqueous media. Macromolecules 46:3125–3131
92. Candau F, Regalado EJ, Selb J (1998) Scaling behavior of the zero shear viscosity of hydrophobically modified poly(acrylamide)s. Macromolecules 31:5550–5552
93. Kujawa P, Audibert-Hayet A, Selb J, Candau F (2004) Rheological properties of multisticker associative polyelectrolytes in semidilute aqueous solutions. J Polym Sci B 42:1640–1655
94. Kujawa P, Audibert-Hayet A, Selb J, Candau F (2006) Effect of ionic strength on the rheological properties of multisticker associative polyelectrolytes. Macromolecules 39:384–392
95. Abdurrahmanoglu S, Can V, Okay O (2009) Design of high-toughness polyacrylamide hydrogels by hydrophobic modification. Polymer 50:5449–5455
96. Abdurrahmanoglu S, Cilingir M, Okay O (2011) Dodecyl methacrylate as a crosslinker in the preparation of tough polyacrylamide hydrogels. Polymer 52:694–699

97. Jiang G, Liu C, Liu X, Zhang G, Yang M, Liu F (2009) Construction and properties of hydrophobic association hydrogels with high mechanical strength and reforming capability. Macromol Mater Eng 294:815–820
98. Jiang G, Liu C, Liu X, Chen Q, Zhang G, Yang M, Liu F (2010) Network structure and compositional effects on tensile mechanical properties of hydrophobic association hydrogels with high mechanical strength. Polymer 51:1507–1515
99. Jiang H, Duan L, Ren X, Gao G (2019) Hydrophobic association hydrogels with excellent mechanical and self healing properties. Eur Polym J 112:660–669
100. Lv X, Sun S, Yang H, Gao G, Liu F (2017) Effect of the sodium dodecyl sulfate/monomer ratio on the network structure of hydrophobic association hydrogels with adjustable mechanical properties. J Appl Polym Sci 134:45196
101. Tuncaboylu DC, Argun A, Sahin M, Sari M, Okay O (2012) Structure optimization of self-healing hydrogels formed via hydrophobic interactions. Polymer 53:5513–5522
102. Can V, Kochovski Z, Reiter V, Severin N, Siebenbürger M, Kent B, Just J, Rabe JP, Ballauff M, Okay O (2016) Nanostructural evolution and self-healing mechanism of micellar hydrogels. Macromolecules 49:2281–2287
103. Molchanov VS, Philippova OE, Khokhlov AR, Kovalev YA, Kuklin AI (2007) Self-assembled networks highly responsive to hydrocarbons. Langmuir 23:105–111
104. Argun A, Algi MP, Tuncaboylu DC, Okay O (2014) Surfactant-induced healing of tough hydrogels formed via hydrophobic interactions. Colloid Polym Sci 292:511–517
105. Gordievskaya YD, Rumyantsev AM, Kramarenko EY (2016) Polymer gels with associating side chains and their interaction with surfactants. J Chem Phys 144:184902
106. Wang C, Wiener CG, Cheng Z, Vogt BD, Weiss RA (2016) Modulation of the mechanical properties of hydrophobically modified supramolecular hydrogels by surfactant-driven structural rearrangement. Macromolecules 49:9228–9238
107. Liu C, Liu X, Yu J, Gao G, Liu F (2015) Network structure and mechanical properties of hydrophobic association hydrogels: surfactant effect I. J Appl Polym Sci 132:41222
108. Algi MP, Okay O (2014) Highly stretchable self-healing poly(N,N-dimethylacrylamide) hydrogels. Eur Polym J 59:113–121
109. Gulyuz U, Okay O (2015) Self-healing poly(N-isopropylacrylamide) hydrogels. Eur Polym J 72:12–22
110. Shang S, Huang SC, Weiss RA (2009) Synthesis and characterization of itaconic anhydride and stearyl methacrylate copolymers. Polymer 50:3119–3127
111. Chen J, Ao Y, Lin T, Yang X, Peng J, Huang W, Li J, Zhai M (2016) High-toughness polyacrylamide gel containing hydrophobic crosslinking and its double network gel. Polymer 87:73–80
112. Xu K, An H, Lu C, Tan Y, Li P, Wang P (2013) Facile fabrication method of hydrophobic-associating cross-linking hydrogel with outstanding mechanical performance and self-healing property in the absence of surfactants. Polymer 54:5665–5672
113. Gao TT, Niu N, Liu YD, Liu XL, Gao G, Liu FQ (2016) Synthesis and characterization of hydrophobic association hydrogels with tunable mechanical strength. RSC Adv 6:43463–43469
114. Akay G, Hassan-Raeisi A, Tuncaboylu DC, Orakdogen N, Abdurrahmanoglu S, Oppermann W, Okay O (2013) Self-healing hydrogels formed in catanionic surfactant solutions. Soft Matter 9:2254–2261
115. Thomas BH, Fryman JC, Liu K, Mason J (2009) Hydrophilic–hydrophobic hydrogels for cartilage replacement. J Mech Behav Biomed Mater 2:588–595
116. Tuncaboylu DC, Argun A, Algi MP, Okay O (2013) Autonomic self-healing in covalently crosslinked hydrogels containing hydrophobic domains. Polymer 54:6381–6388
117. Gulyuz U, Okay O (2014) Self-healing poly(acrylic acid) hydrogels with shape memory behavior of high mechanical strength. Macromolecules 47:6889–6899

118. Lim PFC, Chee LY, Chen SB, Chen B-H (2003) Study of interaction between cetyltrimethylammonium bromide and poly(acrylic acid) by rheological measurements. J Phys Chem B 107:6491–6496
119. Yoshida K, Dubin PL (1999) Complex formation between polyacrylic acid and cationic/nonionic mixed micelles: effect of pH on electrostatic interaction and hydrogen bonding. Colloids Surf A Physicochem Eng Asp 147:161–167
120. Ilekti P, Piculell L, Tournilhac F, Cabane B (1998) How to concentrate an aqueous polyelectrolyte/surfactant mixture by adding water. J Phys Chem B 102:344–351
121. Fundin J, Hansson P, Brown W, Lidegran I (1997) Poly(acrylic acid)−cetyltrimethylammonium bromide interactions studied using dynamic and static light scattering and time-resolved fluorescence quenching. Macromolecules 30:1118–1126
122. Carnali JO (1993) (Polymer/polymer)-like phase behavior in the system tetradecyltrimethylammonium bromide/sodium polyacrylate/water. Langmuir 9:2933–2941
123. Chiappisi L, Hoffmann I, Gradzielski M (2013) Complexes of oppositely charged polyelectrolytes and surfactants – recent developments in the field of biologically derived polyelectrolytes. Soft Matter 9:3896–3909
124. Hansson P (1998) Self-assembly of ionic surfactant in cross-linked polyelectrolyte gel of opposite charge. A physical model for highly charged systems. Langmuir 14:2269–2277
125. Wang C, Tam KC (2002) New insights on the interaction mechanism within oppositely charged polymer/surfactant systems. Langmuir 18:6484–6490
126. Magny B, Iliopoulos I, Zana R, Audebert R (1994) Mixed micelles formed by cationic surfactants and anionic hydrophobically modified polyelectrolytes. Langmuir 10:3180–3187
127. Philippova OE, Hourdet D, Audebert R, Khokhlov AR (1996) Interaction of hydrophobically modified poly(acrylic acid) hydrogels with ionic surfactants. Macromolecules 29:2822–2830
128. Bilici C, Ide S, Okay O (2017) Yielding behavior of tough semicrystalline hydrogels. Macromolecules 50:3647–3654
129. Matsuda A, Sato J, Yasunaga H, Osada Y (1994) Order-disorder transition of a hydrogel containing an n-alkyl acrylate. Macromolecules 27:7695–7698
130. Osada Y, Matsuda A (1995) Shape memory in hydrogels. Nature 376:219–219
131. Tanaka Y, Kagami Y, Matsuda A, Osada Y (1995) Thermoreversible transition of the tensile modulus of a hydrogel with ordered aggregates. Macromolecules 28:2574–2576
132. Uchida M, Kurosawa M, Osada Y (1995) Swelling process and order-disorder transition of hydrogel containing hydrophobic ionizable groups. Macromolecules 28:4583–4586
133. Platé NA, Shibaev VP (1974) Comb-like polymers. Structure and properties. J Polym Sci D Macromol Rev 8:117–253
134. Alig I, Jarek M, Hellmann GP (1998) Restricted segmental mobility in side-chain crystalline comblike polymers, studied by dielectric relaxation measurements. Macromolecules 31:2245–2251
135. Kurt B, Gulyuz U, Demir DD, Okay O (2016) High-strength semi-crystalline hydrogels with self-healing and shape memory functions. Eur Polym J 81:12–23
136. Geng Y, Lin XY, Pan P, Shan G, Bao Y, Song Y, Wu ZL, Zheng Q (2016) Hydrophobic association mediated physical hydrogels with high strength and healing ability. Polymer 100:60–68
137. Zhang H, Han D, Yan Q, Fortin D, Xia H, Zhao Y (2014) Light-healable hard hydrogels through photothermally induced melting–crystallization phase transition. J Mater Chem A 2:13373–13379
138. Nitta K-H, Takayanagi M (2003) Novel proposal of lamellar clustering process for elucidation of tensile yield behavior of linear polyethylenes. J Macromol Sci B Phys B42:107–126
139. Nitta K-H, Takayanagi M (1999) Role of tie molecules in the yielding deformation of isotactic polypropylene. J Polym Sci B 37:357–368
140. Nitta K-H, Takayanagi M (2000) Tensile yield of isotactic polypropylene in terms of a lamellar-cluster model. J Polym Sci B 38:1037–1044

141. Argun A, Gulyuz U, Okay O (2018) Interfacing soft and hard materials with triple-shape-memory and self-healing functions. Macromolecules 51:2437–2446
142. Nerurkar NL, Elliott DM, Mauck RL (2010) Mechanical design criteria for intervertebral disc tissue engineering. J Biomech 43:1017–1030
143. Iatridis JC, Nicoll SB, Michalek AJ, Walter BA, Gupta MS (2013) Role of biomechanics in intervertebral disc degeneration and regenerative therapies: what needs repairing in the disc and what are promising biomaterials for its repair? Spine J 13:243–264
144. Shaw HM, Benjamin M (2007) Structure-function relationships of entheses in relation to mechanical load and exercise. Scand J Med Sci Sports 17:303–315
145. Argun A, Gulyuz U, Okay O (2019) Semi-crystalline, three-segmented hybrid gels with multiple shape memory effect. Macromol Symp 385:1800164